A Y-linked duplication of anti-Mullerian hormone is the sex determination gene in threespine stickleback

Matthew J Treaster, Jenny McCann, Kyra S Solovei, Ryan J Palmieri, Michael A White*

Department of Genetics, University of Georgia, Athens, GA, 30602

Corresponding Author:
Michael A. White
Department of Genetics, University of Georgia
120 Green St,
Athens, GA 30602
whitem@uga.edu

Abstract

Many taxa have independently evolved genetic sex determination where a single gene located on a sex chromosome controls gonadal differentiation. The gene anti-Mullerian hormone (*amh*) has convergently evolved as a sex determination gene in numerous vertebrate species, but how this gene has repeatedly evolved this novel function is not well understood. In the threespine stickleback (*Gasterosteus aculeatus*), *amh* was duplicated onto the Y chromosome (*amhy*) ~22 million years ago. To determine whether *amhy* is the primary sex determination gene, we used CRISPR/Cas9 and transgenesis to show that *amhy* is necessary and sufficient for male sex determination, consistent with the function of a primary sex determination gene. Despite being indispensable for sex determination, we detected low levels of *amhy* expression throughout early development. This indicates the mechanism of sex determination is likely unrelated to overall dosage of *amhy* and its autosomal paralog, *amha*. Threespine stickleback have striking differences in behavior and morphology between sexes. The creation of sex reversed lines allow us to investigate the genetic basis of secondary sex characteristics. Here we show one of the classic traits important for reproductive success, male nuptial coloration, is controlled by both Y-linked genetic factors as well as hormonal factors independent of sex chromosome genotype. This research establishes stickleback as a model to investigate how *amh* regulates gonadal development and how this gene repeatedly evolves novel function in sex determination. Analogous to the four core genotypes model in house mice, sex-reversed threespine stickleback offer a new vertebrate model for investigating the separate contributions of gonadal sex and sex chromosomes to sexual dimorphism.

Introduction

For species that have two discrete sexes, sex determination is the process that designates whether an individual will become male or female [1,2]. While this process is essential to the fitness and survival of a species, it is regulated by a surprising variety of initial

cues and can incorporate a range of extrinsic signals as well as intrinsic genetic factors often located on sex chromosomes [1–3]. Numerous eukaryotic taxa have convergently evolved sex chromosomes, such as the XX-XY system found in mammals, to regulate this critical developmental process [1,2]. Sex chromosomes are derived from a pair of autosomes after one of these autosomes acquires a sex determining (SD) gene [4]. Suppression of recombination around this gene leads to sequence divergence of the two autosomes into a pair of divergent sex chromosomes [4]. Why this recombination suppression occurs is not clear; however, the prevailing model is that suppressed recombination will be selected for to link an SD gene with nearby sexually antagonistic mutations that are beneficial to one sex but detrimental to the other [4–6]. One remarkable observation that has emerged from comparative studies is the SD gene responsible for initiating development of testes or ovaries in their respective sex is incredibly variable [1,7]. How the otherwise well conserved sex differentiation developmental network can be regulated by such a diverse range of SD genes remains poorly understood.

While a wide variety of genes have evolved novel function as sex determination genes, some genes appear predisposed to acquiring this role and have convergently evolved as sex determination genes in distantly related taxa [7]. *Sox3*, the ancestor of the mammalian SD gene *Sry,* also acts as the SD gene in the Indian rice fish (*Oryzias dancena*) [8]. SD genes derived from *dmrt1* are found in birds [9], the African clawed frog (*Xenopus laevis*) [10], and medaka (*Oryzias latipes*) [11,12]. The most prevalent SD gene among vertebrates by far is *anti-Müllerian hormone* (*amh*) [7]. Independently acquired Y-linked copies of *amh* or its dedicated receptor, *amhrII*, have been identified in at least twelve different clades of teleost fish [13–23] as well as in monotremes [24]. These Y-linked copies of *amh* and *amhrII* are presumed to be SD genes in all of these taxa. Although *amh* accounts for over one quarter of identified SD genes in vertebrates, how *amh* controls this critical developmental process and evolves novel function in sex determination is not clear [7].

Amh is a member of the transforming growth factor beta (TGF-β) family of proteins that are shared across vertebrates (Reviewed in [25,26]). *Amh* is unique among TGF-β hormones as it has only one identified type II receptor, *amhrII*, of which *amh* is the only known ligand [27–29]. *Amh* and its receptor were first identified for their role in reproductive tract development in mammals, where secretion of *amh* by the developing testes causes regression of the primordial female reproductive tract, the Müllerian ducts [30]. Disruption of *amh* signaling in teleosts, which lack Müllerian ducts, causes over proliferation of germ cells in the gonad and can interfere with sex determination, even in species were *amh* is not the SD gene [31–33]. This suggests the ancestral function of *amh* is likely in germ cell proliferation and maintenance which, if disrupted, can disrupt sex determination, but how this disruption occurs is not clear. It also is not known whether Y-linked copies of *amh* that have convergently evolved function in sex determination control the downstream network in the same way or if *amh* can regulate sex differentiation through a variety of distinct mechanisms.

Species of stickleback fish (family Gasterosteidae) have multiple, independently evolved sex chromosome systems, making them an ideal model for investigating the origins of sex chromosomes and SD genes [20,34–37]. Two separate duplications of *amh* that are associated with male sex have been identified within stickleback fish. In the genus *Gasterosteus*, *amh* was duplicated from autosome 8 onto autosome 19 approximately 22 million years ago (Mya), leading to the evolution of a Y chromosome [20,38]. An independent duplication of *amh* onto chromosome 20 was identified in the brook stickleback, *Culea inconstans*. This duplication differs from the ancestral copy on autosome 8 by only a handful of single nucleotide polymorphisms (SNPs), suggesting this duplication occurred much more recently than in the genus *Gasterosteus* [22,39]. Consistent with its recent acquisition, the duplicate copy of *amh* is not a fully penetrant SD gene, and its association with male sex varies across populations [39]. This provides a unique opportunity to examine the convergence evolution of *amh* as an SD gene at two dramatically different stages of sex chromosome evolution.

The threespine stickleback (*Gasterosteus aculeatus*) is a powerful emerging model for evolutionary and developmental biology with a robust set of genomic and functional genetic tools [40,41]. Their small size, large clutch sizes, and relatively short generation time make them a highly tractable model for studying the developmental mechanisms of *amh* as an SD gene. Threespine stickleback also have many well-studied sexually dimorphic traits and mating behaviors that have provided substantial insight into the evolution of sexual dimorphism and its effect on fitness [42–63]. Like other members of its genus, threespine stickleback have retained a functional copy of autosomal *amh* on chromosome 8 (hereafter called *amha*) as well as the Y-linked *amhy*. The AMH prodomain and TGF-β signaling domain within *amhy* are conserved (Fig S1), indicating the Y-linked duplicate is likely functional [20]. In addition, *amhy* is expressed in larvae around the time of sex determination, consistent with a role in initiating male development [20]. Beyond this, it is unknown whether *amhy* has a functional role in male sex determination. In this study, we show that *amhy* is both necessary and sufficient for male sex determination in the threespine stickleback, demonstrating that it is the SD gene in this species. We also perform RNA-seq of stickleback embryos and larvae to characterize expression of *amhy* and early transcriptional differentiation of males and females. Our findings establish stickleback fish as a premier model to study both the molecular mechanisms of *amh* based sex determination as well as the convergent evolution of *amh* as a sex determination gene in vertebrates.

Results

CRISPR/Cas9 knockout of *amhy* caused male-to-female sex reversal in XY fish.

If *amhy* is the SD gene in threespine stickleback, it should be both necessary and sufficient for male sex determination. To test this, we first knocked out function of *amhy* in XY fish using CRISPR/Cas9. We designed two sgRNAs targeting exon 1 and exon 3 of *amhy* (Fig 1). We injected stickleback embryos from lab-reared fish derived from two independent marine

118 populations (Port Gardner Bay and Japan Pacific Ocean) with CRISPR ribonucleoprotein (RNP)
119 made with one of the two sgRNAs. 8/17 (47%) of F0 XY fish injected with RNP exhibited male-
120 to-female sex reversal. For all eight XY sex reversed fish, we observed ovaries with all cell
121 types seen in wildtype ovaries (Fig S2).

122 F0 crispants are often mosaic for mutations induced by CRISPR/Cas9 gene editing,
123 which can cause variation in observed phenotypes. To generate non-mosaic F1 gene-edited
124 fish, we used two F0 XY males that had heritable germline mutations in *amhy* but were not sex
125 reversed, indicating they likely did not have *amhy* mutations in cell-lineages important for sex
126 determination. Sperm from these fish were used to fertilize eggs from wildtype XX females. F1
127 offspring from these crosses inherited frameshift mutations in *amhy*, identified by Sanger
128 sequencing (Fig S3). We analyzed five F1 males from one F0 crispant with mutations in exon 1
129 and 21 F1 males from one F0 crispant with mutations in exon 3. All 26 F1 fish exhibited
130 complete male-to-female sex reversal and developed ovaries morphologically and histologically
131 indistinguishable from wildtype XX females (Fig 1C). No F1 XY fish showed development of
132 testis or ambiguous gonad tissue with any visible spermatocyte production. We identified three
133 loss of function alleles in exon 1 of *amhy* (Fig 1A) and one in exon 3 (Fig 1B). In ten F1 fish, the
134 region of *amhy* in exon 3 targeted by CRISPR/Cas9 could not be amplified. PCR of exons 1 and
135 7 showed the presence of these distal portions *amhy*, but PCRs spanning a large putative
136 deletion all failed to amplify, suggesting a chromosomal rearrangement disrupted *amhy* in these
137 fish. As a specific mutation could not be positively identified, these samples were excluded from
138 further analysis and final counts.

139 We analyzed the expression of canonical male differentiation genes *amha* and *dmrt1*
140 and female differentiation genes *foxl2* and *cyp19a1a* using *in situ* hybridization on wildtype and
141 F1 XY *amhy*-KO ovaries (Fig 2, Fig S4). We also analyzed *gsdf* as a positive control, as this
142 gene is expected to be expressed in somatic gonadal cells of both sexes [64]. Both wildtype and
143 sex reversed ovaries showed expression of *foxl2* and *cyp19a1a* in somatic cells. Expression of

144 *amha* and *dmrt1* was minimal and restricted to oocytes when present as has been observed in
145 some species of fish [21,65–68]
146 Knockout of *amh* or *amhrII* in teleost species without amh-based sex determination has
147 caused male-to-female sex reversal, including in lab strains of zebrafish which lack sex
148 chromosomes (reviewed in [69]) and medaka which have an XX-XY system with a *dmrt1*
149 derived sex determination gene [31]. Thus, it is possible that off-target mutations of the
150 homologous *amha* could contribute to the sex reversal observed in F1 *amhy* mutants. While
151 both sgRNAs have multiple mismatches to their homologous region in *amha*, we verified that all
152 F1 XY *amhy*-KO females did not have mutations within *amha* by sanger sequencing (Fig S5).
153 This demonstrates that the sex reversal phenotype was not caused by mutations of *amha*. We
154 also investigated whether the sex reversal phenotype was caused by a mutation at an unknown
155 autosomal locus. This autosomal mutation must be dominant since we observed male-to-female
156 sex reversal in heterozygous XY F1 fish. F1 XX siblings of sex reversed XY fish would also be
157 heterozygous for this mutation, and half of their F2 XY progeny would be sex reversed. We
158 crossed two F1 XX PG females with wildtype XY males and phenotyped F2 offspring for sex
159 reversal. All 16 16 F2 XY fish were phenotypically male, indicating that sex reversal in F1 XY
160 *amhy*-KO fish was not caused by an off-target autosomal mutation.
161
162 **Introduction of an *amhy* transgene caused female-to-male sex reversal in XX fish.**
163 To determine if *amhy* is sufficient for male sex determination, we created a construct
164 (pT2-5amhy2.5,Xla.Ef1a:EGFP) containing an 11 kb region of the Y chromosome which
165 includes *amhy*, 5 kb of upstream sequence, and 2.5 kb of downstream sequence (Fig S6F). By
166 including the surrounding non-coding sequences, we aimed to recapitulate the endogenous
167 expression patterns of *amhy.* An Xla.Ef1a:EGFP cassette downstream of *amhy* was included to
168 facilitate the screening of injected embryos for transgene integration. These components were
169 flanked by *Tol2* transposon sequences to facilitate random integration into the genome by the

170 Tol2 transposase [70,71]. 16 F0 XX fish showed positive GFP expression and successful
171 transgene integration, detected through PCR genotyping (Fig 3D). At reproductive age, all 16 F0
172 XX *Tg(amhy,EGFP)* were female-to-male sex reversed, developing testes rather than ovaries
173 (Fig 3A). All 10 control F0 XX fish injected with the control Xla.ef1a:EGFP transgene showed
174 positive presence of the transgene, but did not show any signs of sex reversal and developed
175 cytologically normal ovaries (Fig 3B). We also analyzed the expression of *amha, dmrt1, foxl2*,
176 *cyp19a1a,* and *gsdf* using *in situ* hybridization on wildtype and F0 XX *Tg(amhy,EGFP)* testes
177 (Fig 2, Fig S7). Both wildtype and sex reversed testes showed strong expression of *amha* and
178 *dmrt1* in somatic cells and no discernable expression of *foxl2* or *cyp19a1a*.
179 We attempted to constitutively express *amhy* using a synthetic exon-only coding
180 sequence with an N-terminus FLAG tag joined to a 3' EGFP by a P2A self-cleaving peptide
181 [72,73]. Plasmids were made using the *D. rerio* ubiquitin promoter [74] or the *X. laevis* ef1a
182 promoter [75] to drive expression of the amhy,EGFP construct (Fig S6). Transgenes with the
183 respective promoter driving expression of only EGFP were used as controls. While somatic
184 EGFP expression was observed with both control transgenes indicating these promoters can
185 drive expression in stickleback, neither the Dre.Ubi:amhy,EGFP nor the Xla.Ef1a:amhy,EGFP
186 transgene produced any larvae with visible somatic EGFP, indicating that the *amhy* transgenes
187 were failing to integrate or be actively expressed in any embryos. We hypothesize that the
188 failure to constitutively express *amhy* may be due to cytotoxicity of extremely high and
189 widespread expression of *amh* using these non-native, constitutive promoters.
190

191 **Sex reversed *amhy* mutants produce viable gametes but are subfertile.**

192 Sex-reversed XY *amhy*-KO females produced mature oocytes and became gravid, but
193 they were subfertile compared to wildtype females. To assess fertility, we crossed a three F1 XY
194 *amhy*-KO females to wildtype XY males. These clutches all showed extremely low viability rates,
195 between 2% and 6% (Table S1), measured by presence of a gastrula and active epiboly 12 to

24 hours after fertilization (haf). One of the three F1 fish was crossed four additional times and showed improvement in viability with the subsequent crosses. The viability rates of the fourth and fifth cross were 78% and 79% respectively, producing a total of 148 viable F2 eggs (Table S1). Three days after fertilization, 50 of the 148 eggs had arrested development. We were able to genotype 48 of the failed embryos. Three-quarters of these (36) carried no X chromosome and both the paternally transmitted Y chromosome (Y^p) and the maternally transmitted *amhy*-KO Y chromosome (Y^m) (Fig 4). The remaining embryos were reared to adulthood and 92 were genotyped for their sex chromosome complement. No adult YY fish were observed, indicating that the YY genotype is embryonic lethal due to the missing X chromosome. XY^m females were found to transmit the X and Y^m chromosome with equal frequency, indicating there was not any biased transmission of the X or Y chromosome during female meiosis (36 Y^pY^m embryos out of 148 total does not deviate from a 1:4 Mendelian ratio; chi-squared = 0.0360; p = 0.8494; of the 92 adult F2s genotyped 36 XX, 27 XY^p , and 29 XY^m does not deviate from the expected 1:1:1 ratio; chi-squared = 1.457; p = 0.4827). Subfertility also extended to second generation sex-reversed XY females. We crossed 11 F2 females with wildtype XY males. The clutch size did not differ significantly between XY^m and XX females (Fig 4C; Table S2). However, the viability rate was substantially lower in the F2 XY^m females, similar to the F1 generation (Fig 4D, Table S2). Two XY^m F2 females were also eggbound and were unable to be stripped of eggs.

Female-to-male sex reversed F0 XX fish had varied fertility. We initially dissected eight F0 XX *Tg(amhy,EGFP)* males at 6 months post fertilization. Seven of these XX males had small, underdeveloped testes, whereas one had testes morphologically resembling those of a fertile, wildtype male. Despite its mature morphology, the testis was composed only of premeiotic spermatogonia, immature round spermatids, and no mature sperm (Fig 3A). Crosses with this male only had a 3% viability rate, suggesting the XX male was not reproductively mature. Of six XY fish injected with the control Ef1a:EGFP transgene that were dissected at six months, only two had testes that appeared reproductively mature, and histology of these testes

222 also lacked mature sperm. XX females injected with the control transgene were also not fully
223 mature (Fig 3B).
224 We then assessed fertility of transgenic fish at 12 months of age to ensure the males
225 had adequate time to fully mature. At this age, XY *Tg(EGFP)* control fish showed nuptial
226 coloration, and both XX and XY *Tg(amhy,EGFP)* fish were reproductively mature. We analyzed
227 eight additional F0 XX *Tg(amhy,EGFP)* males at 12 months post fertilization. Three of these
228 males had morphologically and histologically normal testes with fully mature sperm (Fig 3A).
229 These three males showed normal viability rates when crossed with wildtype XX females (78
230 viable of 97 total eggs, 84 viable of 89 total eggs, and 231 viable of 235 total eggs). One male
231 also produced offspring with somatic GFP expression at a very low frequency (16/231)
232 indicating a heritable germline integration of the transgene had occurred. The remaining five
233 males had hypotrophic testes, so no crosses were performed with these males. Histology of the
234 hypotrophic testes was abnormal and did not show any clearly identifiable germ cells (Fig 3A).
235 This phenotypic variation could be a result of variable *amhy* expression influenced by transgene
236 copy number and insertion location.
237
238 **Male nuptial coloration is present in both sex reversed genotypes**
239 Male nuptial coloration is one of the most prominent sexually dimorphic characteristics in
240 threespine stickleback. During their breeding season, males from many stickleback populations
241 develop throats and dark blue eyes and bodies [76]. To investigate the separate contributions of
242 gonadal and genotypic sex on this trait, we compared coloration in mature sex reversed XY
243 *amhy*-KO females and XX *Tg(amhy,EGFP)* males to wildtype XX and XY fish (Fig 5). Nuptial
244 coloration is prominent in XY males by one year post hatching. While neither *amhy* mutant
245 genotype fully recapitulates wildtype XY male coloration, both XX males and XY females show
246 elements of male nuptial coloration and are distinct from wildtype XX females. In XX males,
247 nuptial coloration was present in all three fertile males, but not in any males with hypotrophic

248 testes. Together, these findings show that nuptial coloration is a product of both sex
249 chromosome genotype and gonad identity.
250
251 ***amhy* does not have distinct expression timing relative to *amha***
252 Since Amh shows high specificity for its dedicated receptor, AmhrII, [27–29] we predicted
253 that *amhy* would be functionally constrained regarding coding sequence evolution and would
254 instead evolve novel function through regulatory changes. We investigated the degree of
255 sequence conservation within putative regulatory regions (2 kb upstream and downstream of
256 the coding sequence), of *amhy* relative to *amha*. We also compared sequence similarity
257 between *amha* and the autosomal *amh* in the ninespine stickleback (*Pungitius pungitius*). The
258 divergence time between threespine and ninespine stickleback is approximately 26 Mya [77],
259 similar to the 22 Mya divergence time between the threespine *amha* and *amhy* [20]. There was
260 less sequence identity between the coding sequences of threespine *amha* and *amhy* than
261 between threespine *amha* and ninespine *amh* (Fig 6, Table 1). This is consistent with weaker
262 purifying selection acting on the Y chromosome due to a lack of recombination [78]. This was
263 also supported by a higher dN/dS value between threespine *amha* and *amhy* than between
264 threespine *amha* and ninespine *amh*. The sequence identity of upstream and downstream
265 regions was much lower between *amha* and *amhy* than between *amha* and ninespine *amh*,
266 indicating *amhy* has undergone significant regulatory evolution since its duplication onto the Y
267 chromosome, which may cause differences between *amha* and *amhy* expression.
268 To determine whether expression of these genes differ throughout development, we
269 sequenced the total transcriptomes from prehatching embryonic stages 17 (early
270 somitogenesis, ~43 haf), 20 (onset of pigmentation, ~73 haf), and 23 (completion of yolk sac
271 circulation, ~122 haf) as well as larvae 0, 4, and 8 days after hatching (dah), where hatching
272 occured around 200 haf [79]. The earliest identified morphological difference between male and
273 female threespine stickleback is a difference in primordial germ cell count at 3 to 4 dah [80]. Sex

determination should begin sometime prior to this stage. We predicted that the unique regulatory architecture of *amhy* resulted in earlier expression timing relative to *amha.* Thus, *amhy* would be expressed at higher levels relative to *amha* early in development in order to initiate sex determination. As the gonad differentiates, *amha* expression should increase relative to *amhy* due to the canonical role of *amh* in male differentiation. This pattern has been observed in Japanese flounder [15] and Patagonian pejerrey [13] which also have *amhy* SD genes. Contrary to our prediction, we found that *amhy* expression was substantially lower than *amha* at all observed timepoints pre- and post-hatch (Fig 7B). This difference was still present after scaling read counts for differences in transcript length which is not accounted for by normalized read counts (Table S3). We found *amhy* expression trended towards higher expression at later developmental stages, consistent with a role in sex determination. However, this difference was not significant (anova $p = 0.0769$). We then hypothesized that male sex determination could be initiated by a higher overall dose of *amhy* when expressed simultaneously with *amha.* We compared *amha* and transcript length adjusted *amhy* normalized read counts at each stage and found no significant difference in total *amh* dosage between males and females at any timepoint (Table S3), suggesting dosage alone is not a mechanism for initiating male differentiation. Combined, our results indicate the unique regulatory elements that evolved for *amhy* do not increase early expression of *amhy*. Instead, they may alter expression level of *amhy* at other developmental stages and/or change spatial expression patterns, contributing to its new function in sex determination.

Sex differentiation genes are not differentially expressed between males and females early in development

Following sex determination, we expected to see divergence in the expression of overall male and female transcriptomes. However, principal component analysis of autosomal gene expression indicated that male and female larvae had similar expression profiles. Autosomal

300 genes were clustered by developmental time rather than separating by sex at any stage of
301 development (Fig 7A). Only sex chromosomes showed clear separation by both sex and
302 developmental time (Fig S8), since the X chromosome is expressed two-fold higher in females,
303 relative to males, and the Y chromosome is only expressed in males. The overall lack of sex-
304 specific expression on the autosomes suggests that many aspects of sex differentiation occur
305 well after the earliest noted phenotypic difference between males and females: the proliferation
306 of germ cells in the primordial gonad at 3 to 4 dah [80].

307 We examined whether any developmental stages had genes that were significantly
308 differentially expressed between males and females. Many male and female differentiation
309 genes are highly conserved across vertebrates [2] and should also be expressed during
310 development of the threespine stickleback. For instance, we expected differential expression of
311 key transcription factors canonically involved in differentiation, including the male biasing factors
312 *dmrt1* and *sox9b* or the female biasing factors *foxl2a*, followed by divergence of downstream
313 genes such as the aromatase enzyme *cyp19a1a* and the TGF-b hormones *amha* and *gsdf*. In
314 total, we found 464 differentially expressed genes (DEGs) between males and females on the
315 autosomes (File S1). Key regulators of differentiation should be differentially expressed
316 throughout development and into adulthood in order to actively maintain gonadal fate [2].
317 However, 438 of the DEGs were only differentially expressed in a single stage (File S1),
318 suggesting these genes do not play a substantial role in sex differentiation. Additionally, while
319 we expected to see an increase in the number DEGs over time due to activation of male and
320 female specific gene networks, the number of DEGs was highest at stage 17 (152 DEGs),
321 decreasing in later stages until a small increase from 4 dah (40 DEGs) to 8 dah (72 DEGs) (Fig
322 S9). None of the canonical differentiation genes of interest were differentially expressed
323 between males and females at any timepoint examined in this study (Fig 7). Male differentiation
324 genes *dmrt1* and *amha* and female differentiation genes *foxl2* and *cyp19a1a* were differentially
325 expressed in adult gonads of both wildtype and sex reversed fish, indicating their function in

326 differentiation are conserved (Fig 2, Fig S4, Fig S7). Of the identified DEGs, only a small
327 handful have known associations with gonadal function, development, or differentiation. Two
328 genes associated with germ cell specification and maintenance [81], *ddx4* and *piwil1*, showed
329 female biased expression at 8 dah (Fig 2C). Interestingly, *amhrII,* which shows female biased
330 expression in embryonic mouse gonads [82], was also expressed more highly in females at 8
331 dah. While *cyp19a1a* was not differentially expressed, the steroidogenic enzyme *hsd17b1*,
332 which plays a role in both estrogen activation and androgen inactivation [83] and acts as the SD
333 gene in *Seriola* fishes [84], showed female biased expression at 8 dah. A lack of differential
334 expression in many of these key genes indicates that gonad differentiation occurs after 8 dah.
335 We identified some other DEGs that have known reproductive functions in other
336 vertebrates but do not have clear connections to sex differentiation and are only differentially
337 expressed at a single timepoint. Gonadotropin-releasing hormone II receptor (LOC120811940)
338 has known roles in the stimulating steroidogenesis in both testes and ovaries across mammals
339 [85] and had male biased expression at stage 17 (logFC = 2.74, adjusted P = 1.4E-3). TGF-beta
340 3 hormone is expressed more highly in male mice during gonadogenesis [86], and a TGF-beta 3
341 proprotein like gene (LOC120807995) was expressed slightly higher in females at stage 17
342 (logFC = -0.63, adjusted P = 0.044). *Piwil2*, another germ cell associated gene [81], was
343 expressed higher in males at stage 20 (logFC = 1.72, adjusted P = 3.2E-3). *Cdc25b* is
344 expressed at low levels in mouse ovaries and testes [87] and was male biased at stage 23
345 (logFC = 0.52, adjusted P = 0.012). Separin/separase (*espl1*) has known roles in mitotic and
346 meiotic chromosome segregation [88] and was expressed at higher levels in 8 dah females
347 (logFC = -0.56, adjusted P = 1.2E-4). Additional work will be necessary to understand what
348 function, if any, these genes have in threespine stickleback gonad development.
349

350 **Discussion**

351 ***amhy* is the sex determination gene in threespine stickleback fish**

352 Our findings demonstrate that *amhy* is the SD gene in threespine stickleback, as it is
353 both necessary and sufficient for sex determination (Table 3). Independently derived *amhy*
354 genes have been functionally demonstrated to have a role in sex determination in three other
355 clades of teleost; however, threespine stickleback offers a novel perspective as their *amhy* is
356 more diverged, and genetic sex determination is more canalized in this species. Nile tilapia and
357 Japanese flounder have only one and nine SNPs, respectively, that differentiate their X- and Y-
358 linked copies of *amh* [15,16], and *amhy* in Patagonian pejerry shares 94% nucleotide identity
359 with its autosomal paralog [13]. In all three of these species, genetic sex determination can be
360 overridden to varying degrees by temperature [89–91]. In contrast, the threespine stickleback,
361 *amha* and *amhy* only share 78% nucleotide identity (Table 1). There is no evidence that
362 temperature can disrupt sex determination in threespine stickleback, and occurrences of sex
363 reversed or intersex stickleback in wild populations is rare [92,93]. This indicates that genetic
364 sex determination is highly canalized in threespine stickleback and less susceptible to
365 environmental signals that many other teleost species, making stickleback a robust model to
366 investigate how *amh* regulates gonadal development. Comparative studies across these taxa
367 will be invaluable for understanding how *amh* repeatedly evolves this novel function, and the
368 presence of an independently derived male associated *amh* duplication in the closely related
369 brook stickleback [22,39] makes the stickleback family an especially powerful tool for studying
370 the convergent evolution of *amh* as an SD gene.
371

372 **Potential mechanisms of sex determination in stickleback**

373 Germ cell density has been shown to affect sex determination in several teleost species,
374 with the male fate associated with lower germ cell count and the female fate with a higher count.
375 Common lab zebrafish strains are undifferentiated gonochorists, where all individuals begin
376 ovary development, but the gonad transitions early in males to a testis [94]. Complete ablation
377 of germ cells causes zebrafish to undergo male development [95], and a threshold of germ cells

378 at the time of gonadal differentiation is necessary to sustain ovary development [96]. *O. latipes*,
379 like sticklebacks, are differentiated gonochorists where either testis or ovary development
380 begins from a common undifferentiated primordium [97]. Ablation of germ cells in XX *O. latips*
381 causes female-to-male sex reversal [98], and overproliferation of germ cells in XY fish causes
382 male-to-female sex reversal [99]. The association of germ cells with sex has also been
383 observed outside of teleosts in the red eared slider turtle (*Trachemys scripta elegans*) which has
384 temperature dependent sex determination. Embryos incubated at female promoting
385 temperatures have higher germ cell counts than those incubated at male promoting
386 temperatures, and depleting germ cells at intermediate temperatures biased the sex ratio
387 towards males [100]. This suggests the presence of a widely conserved, ancestral mechanism
388 in vertebrates by which germ cell density governs gonad differentiation. A new duplication of
389 *amh* could increase overall *amh* dosage, reducing germ cell proliferation to co-opt this
390 underlying mechanism and become a male determining gene.

391 Consistent with this mechanism, we found evidence that *amhy* is expressed in
392 threespine stickleback when germ cell proliferation diverges in males and females. While *amhy*
393 levels were low at all stages observed, *amhy* expression was highest in post hatching stages
394 where differences in germ cell proliferation between males and females are first observable in
395 the developing gonad [80]. We also found increased expression of germ cell specific genes (e.g.
396 *ddx4* and *piwil1*) in females at 8 dah, corroborating previous histological observations of
397 increased germ cell proliferation in female stickleback gonads beginning at 3 dah [80].
398 Overexpression of *amh* in mice [101] and chicken [102] causes reduced germ cell count and
399 gonad size. Studies misexpressing *amh* in telesots have primarily focused on sex determination;
400 however, gonadal hypertrophy observed in *amh* knockouts in other teleosts [31,33] alongside
401 gonadal hypotrophy with a lack of mature germ cells observed in some XX *Tg(amhy,EGFP)*
402 males in this study demonstrate the conserved function of *amh* suppressing germ cell
403 proliferation in stickleback and other teleosts.

404 Somatic cells may also be affected by *amhy* in other ways. In mice, low concentrations
405 of Amh promote proliferation and growth factor production in somatic cells, while increased
406 concentrations induce apoptosis [103]. Altering somatic cell proliferation could lead to
407 differences in the levels of hormones and growth factors that they produce, shaping gonadal
408 development. While Amh is not necessary for initial gonadal differentiation, it is important to
409 maintaining Sertoli cell fate in fetal mice [104]. Estrogen production in somatic cells also plays a
410 major role in sex differentiation and ovary development in teleosts (reviewed in [105,106]). In
411 tilapia, Amh signaling directly inhibits *cyp19a1a* production via Smad transcription factors [107].
412 While we did not detect a difference in *cyp19a1a* expression between males and females in
413 embryos or larvae, it was expressed more highly in adult ovaries than in testes, so *amhy* could
414 play a reinforcing role later in development to suppress estrogen synthesis in males. As we
415 were unable to isolate embryonic gonadal tissue for expression analysis, our results are
416 currently limited to characterizing total expression in the whole embryo. *Amh* can be expressed
417 in other developing tissues, such as the brain and heart [108,109]. If this is also the case in
418 threespine stickleback, this would obscure the true *amhy* to *amha* expression ratio in the gonad.
419 Further research characterizing the expression of *amha* and *amhy* in stickleback at spatial and
420 single cell levels will be essential for understanding how *amhy* functions in the developing
421 stickleback gonad.

422 The evolutionary changes that have given rise to novel function of *amhy* in stickleback
423 sex determination remain unclear. It is clear that substantial regulatory evolution has taken
424 place following the duplication of *amh* onto the Y chromosome; however, this regulatory
425 evolution has not lead to earlier or higher expression of *amhy* relative to *amha* as we initially
426 predicted. While we suspect a more detailed study of *amha* and *amhy* expression at tissue and
427 cell specific levels will lend insight into the role of this regulatory evolution, we also should not
428 rule out the significance of coding sequence evolution for *amhy*. In Nile tilapia, *amhy* expression
429 is lower than the X-linked *amh* throughout development, and misexpression of *amhy* but not

430 *amh* induces male sex determination [16]. This implies that the single missense SNP between
431 *amh* and *amhy* in tilapia is important to the function of *amhy* in sex determination. In Spotted
432 knifejaw (*Oplegnathus punctatus*), a Y linked copy of *amhrII* shows higher affinity for binding
433 *amh* than its X linked paralog [23]. In zebrafish which lack *amhrII*, *amh* may instead use the type
434 II TGF-β receptor *bmpr2a* [110,111]. Mutations that increase the stability of Amhy, increase its
435 affinity for the receptor, AmhrII, or promote interaction with a non-canonical receptor could also
436 affect gonadal development.
437
438 **Sex differentiation occurs later than anticipated**
439 We observed no differential expression in canonical vertebrate sex differentiation genes,
440 including *dmrt1, sox9b, foxl2a,* and *cyp19a1a.* While the order and timing of expression varies
441 across taxa, these core genes are reliably differentially expressed between males and females
442 before the onset of morphological gonadal differentiation [112–114]. This indicates that there is
443 some delay between the initial establishment of germ cell differences between males and
444 females and the later differentiation of the primordial gonad into either a testis or ovary. We
445 propose that sex determination in threespine stickleback occurs in two phases. In the early
446 critical period of sex determination, germ cell proliferation in the undifferentiated gonad diverges
447 between males and females due to the presence of *amhy* in males. Then, during the sensitive
448 period of gonadal differentiation, the difference in germ cell count between individuals dictates
449 gonadal fate, marking the end of the sex determination and the beginning of differentiation.
450 Unlike *Sry* in mammals which is expressed in a brief window and directly initiates gonadal
451 differentiation [115], *amhy* in stickleback appears to be expressed throughout this early period of
452 germ cell proliferation. These two phases of germ cell proliferation followed by gonad
453 differentiation are also present in other species with SD genes including Nile tilapia (reviewed in
454 [116]), and medaka (reviewed in [97]) as well as species without SD genes such as red eared
455 slider [100] where germ cell proliferation is affected by temperature. This suggests that this two-

456 phase system of differential germ cell proliferation followed by gonadal differentiation is broadly
457 conserved across vertebrates, but what combination of environmental and/or genetic factors
458 influences germ cell proliferation has changed between taxa. The ability of *amh* to immediately
459 integrate with this preexisting sex determination network through its existing function in
460 regulating germ cell proliferation along with possible reinforcing roles in regulating somatic cell
461 identity and estrogen synthesis would explain the prevalence of *amh* as an SD gene.
462

463 **Fertility of sex reversed threespine stickleback**

464 Both XY *amhy*-KO females and XX *Tg(amhy,EGFP)* male sex reversed fish were fertile
465 in our study. Fertility of sex reversed mutants is not uncommon in other teleost species;
466 however, it is often observed in species with younger or less diverged sex chromosomes. In
467 these instances, the X and Y chromosomes contain a similar complement of genes. In medaka,
468 the Y specific region is 280 kb and the only functional gene it contains is the sex determining
469 *dmrt1by* [12]. In Nile Tilapia, the sex determining region on linkage group 23 is 1.5 Mb and
470 contains 51 annotated genes, including the sex determining *amhy* [117]. In both species, sex
471 reversed fish are fertile and YY offspring are viable [11,118]. In contrast, the threespine
472 stickleback Y chromosome has a ~15 Mb non-recombining region [20]. Within this region, the Y
473 chromosome has lost half of the almost 1200 ancestral gametologs and has accumulated many
474 Y-specific genes not present on the X chromosome [20]. Sex chromosome-specific gene
475 content evolution could lead to improper expression in the opposite sex, affecting
476 gametogenesis. Given this divergence, the ability of both XY *amhy*-KO females and XX
477 *Tg(amhy,EGFP)* males to reproduce is surprising. In mouse, reduced fertility of XY females is a
478 result of meiotic errors between the X and Y chromosomes as well as the effect of aberrant Y-
479 chromosome genes in the ooplasm on early development (Reviewed in [119]). As clutch size in
480 XY females did not differ from XX siblings and some crosses from XY females have normal
481 viability, it seems unlikely that widespread meiotic failure occurs in XY female stickleback.

Furthermore, it is clear that Y chromosome transcripts or dosage differences from X chromosome genes do not prevent embryo development. Threespine stickleback are batch spawners that produce multiple clutches of eggs over a single breeding season [76]. If ovulated eggs are not passed, they can become overripe and inviable [120,121]. Overripe eggs can also harden and obstruct the fish, causing them to become eggbound. Many of the clutches from XY *amhy*-KO females had this hardened, overripe appearance that is uncommon in our lab-reared, wildtype fish. In addition, some XY females we attempted to cross had no cloaca dilation and were eggbound. We suspect that subfertility of XY females is not due to an inability to produce viable eggs, but due to an inability to pass these eggs once mature. While wildtype fish can pass eggs on their own and begin another cycle of ovulation, XY females retain these eggs until they are manually removed. Repeated and frequent crossing would prevent overripe eggs from building up and allow the harvest of freshly ovulated, viable eggs. Hormones produced by the gonad and pituitary gland appears to play a role in egg maturation and overripening for stickleback [121,122], so while XY females are histologically similar to XX females, variation in hormone production could inhibit proper production and release of eggs.

The mammalian Y chromosome has several genes essential for spermatogenesis and sperm development [123–127]. Single cell sequencing has shown that many Y-specific genes are expressed throughout spermatogenesis in stickleback [128], but these genes are apparently not essential for this process. Several XX *Tg(amhy,EGFP)* males from this study had testes with many fully mature spermatozoa that were able to fertilize eggs and generate viable progeny at similar rates to wildtype sperm. This raises a question of the importance of the Y chromosome to fitness and reproduction. Testes from fertile XX males did not show an obvious reduction in sperm number indicating that widespread meiotic arrest does not occur in XX males. Stickleback are external fertilizers in which sperm competition frequently occurs [129]. Variation in sperm morphology [130] and motility [131] can contribute to reproductive success, so there may be differences in sperm function that our *ex vivo* fertilization assays do not capture. Some

508 XX *Tg(amhy,EGFP)* males did have hypotrophic testes with a reduction in identifiable germ
509 cells, but since this phenotype was not universal, we suspect that variation in transgene copy
510 number and insertion location led to overexpression of *amhy* in these fish. The germline
511 *Tg(amhy,EGFP)* offspring we produced will allow us to determine if this phenotypic variation
512 exists in a consistent genetic background.
513

514 **A four core genotypes stickleback model**

515 Sex chromosomes impact a wide range of traits outside of fertility that are still critical to
516 fitness. By comparing XY males and XX females to sex reversed XY females and XX males, the
517 four core genotypes mouse model has allowed researchers to dissect the role of genotypic and
518 gonadal sex to a number of behavioral and physiological sex differences in mammals (reviewed
519 in [132,133]) including mating behavior [134] and parental care [135]. The creation of
520 reproductively mature XX males and XY females in this study offers a new vertebrate model to
521 study the separate contributions of gonadal sex and sex chromosomes to sexual dimorphism.
522 Many traits are sexually dimorphic in the threespine stickleback, including shape and
523 size of the head and body [42–45], bony armor features [42,43], and brain size [46,47] as well
524 as feeding behaviors [48,49] and boldness [50]. Male stickleback also show complex courtship
525 and mating behavior [51,52] and male-only paternal care [53], while females show a variety of
526 mate choice preferences [54–59]. Male nuptial coloration is a particularly interesting trait, as
527 strong coloration is beneficial for courtship [59,60], but has a cost of increased risk of predation
528 [61,62]. Therefore, sexually antagonistic selection would select for stronger, more conspicuous
529 coloration in males and inconspicuous coloration in females. Androgens, secreted from the
530 gonads, are shown influence nuptial coloration in stickleback [63]. These observations are
531 supported by the presence of nuptial coloration in XX males in our study, which lack all Y-linked
532 genes, but have functioning testes. In contrast, male nuptial coloration in XY females that lack
533 testes shows that there are also Y-linked factors that contribute to nuptial coloration independent

534 of gonadal sex. Future research with the four core genotypes stickleback will provide many
535 insights into the genetic basis of sexual dimorphism and how sexually antagonistic selection
536 shapes the evolution of sex chromosomes.
537
538 **Methods**
539 All experiments used lab-derived progeny from wild-caught threespine stickleback fish
540 from Port Gardner Bay (Washington, USA) and Japan Pacific Ocean (Akkeshi, Japan). All
541 procedures were approved by the University of Georgia Animal Care and Use Committee
542 (protocols A2021 07-031-Y3 and A2024 08-009-Y1). We collected fish from Washington State
543 over multiple years using Scientific Collection Permit numbers 21-122, 22-150, 23-147, and 24-
544 143.
545
546 **CRISPR/Cas9 knockout of *amhy***
547 We microinjected stickleback embryos following standard procedures [40], with the
548 addition of KCl to the injection mix at a final concentration of 0.2 M [136]. Cas9 protein was
549 purchased from QB3 MacroLab (University of California, Berkeley). Synthetic sgRNAs were
550 designed using CHOPCHOP [137–139] and purchased from Synthego: amhy_sgRNA_77r (5'-
551 GATCAGCTGCTGTCCATGCA-3') and amhy_sgRNA_600r (5'- GGTCCTCTCTCGTCTTCGTT -
552 3'). We combined Cas9 protein and sgRNA at a final concentration of 10 μM each and
553 incubated for at least ten minutes at room temperature to allow the ribonucleoprotein (RNP) to
554 form. The injection mix was made to a final concentration of 4 μM RNP.
555
556 **Synthesis of constructs and transgenesis**
557 Plasmids pBT2 [140], pUbi:Switch [74], and pCS-zT2TP [8] were kindly shared by Mary
558 Goll. Plasmid pT2AL200R150G [70] (referred to as pT2Xla.Ef1a:EFGP) was kindly shared by
559 Tyler Square and Craig Miller. We purchased a synthetic amhy,EGFP construct from TWIST

560 Bioscience (San Francisco, CA, USA). This construct consisted of a Kozak consensus
561 sequence (5'-GCCGCCACCATGG-3'), N-terminus flag tag, the threespine stickleback *amhy*
562 coding sequence, a P2A self cleaving peptide [72,73], EGFP, and an SV40 poly(A) sequence,
563 all flanked by 5' BamHI and 3' NotI restriction sites to facilitate cloning. We performed all
564 restriction digests were following the manufacturer's guidelines (New England Biolabs). We
565 isolated all of the plasmids using a Monarch Plasmid Miniprep Kit (NEB #T1010) and gel
566 purified all DNA fragments using the Monarch Gel Extraction kit (NEB #T1020). DNA fragments
567 were ligated using T4 DNA Ligase following manufacturer recommended protcols (NEB
568 #M0202). We transformed all plasmids into DH10B competent cells (Thermo Scientific EC0113).
569 All plasmids were sequenced by Azenta Life Sciences (South Plainfield, NJ, USA) (File S2).

570 We assembled each construct as follows:

571 1. pT2Dre.Ubi:amhy,EGFP: The *D. rerio* ubiquitin promoter was excised from
572 pUbi:Switch and cloned into pBT2 using XhoI and BamHI. The synthetic amhy,EGFP
573 construct was excised from pTwist_amhy-P2A-EGFP and cloned into the
574 intermediate pT2Dre.Ubi backbone using BamHI and NotI.
575 2. pT2Dre.Ubi:EGFP: the *D. rerio* ubiquitin promoter was excised from pUbi:Switch and
576 cloned into pT2Xla.Ef1a:EGFP using XhoI and BamHI.
577 3. pT2Xla.Ef1a:amhy,EGFP: the synthetic amhy,EGFP construct was excised from
578 pT2Dre.Ubi:amhy,EGFP and cloned into pT2Xla.Ef1a:EGFP using BamHI and BglII.
579 4. pT2-5amhy2.5,Xla.Ef1a:EGFP: an 11.5 kb region of the Y chromosome containing
580 *amhy* along with 5 kb of upstream and 2.5 kb downstream DNA was excised from
581 bacterial artificial chromosome STB26-N21 from the CHORI-215 library [141] and
582 cloned into pBT2 using BamHI and XhoI. The Xla.Ef1a:EGFP cassette was excised
583 from pT2Xla.Ef1a:EGFP by digestion with XhoI and HpaI and ligated into the
584 intermediate pT2-5amhy2.5 plasmid following digestion with XhoI and SwaI.

585 We synthesized Tol2 mRNA using the mMessage mMachine SP6 Transcription kit
586 (Invitrogen AM1340) and purified the product with the MEGAclear Transcription Clean-Up Kit
587 (Invitrogen AM1908). We injected stickleback embryos were as in [40] with the addition of KCl to
588 a final concentration of 0.2 M [136]. All embryos were screened for EGFP expression five to
589 seven days after injections before hatching had occurred. We removed all embryos without
590 discernable somatic EGFP fluorescence.
591
592 **Genotyping and sanger sequencing**
593 We extracted DNA from fin clips or whole embryos using a HotSHOT isolation protocol
594 [142]. We performed all PCR reactions on an Analytik Jena Biometra Tone in a total volume of
595 20 µl using 0.8 µL of genomic DNA, 0.2 µM each primer, 0.2 mM each dNTPs, 0.5 units
596 DreamTaq DNA polymerase (Thermo Scientific EP), and 2 µl 10x DreamTaq Green Buffer with
597 20 mM $MgCl_2$. We genotyped fish for sex using the sex-linked marker *idh* [38] with the following
598 cycling conditions: 1 cycle of 95°C for 2 min; 30 cycles of 95°C for 30 s, 57.3°C for 30 s, and
599 72°C for 30 s; 1 cycle of 72°C for 5 minutes. All other reactions used: 1 cycle of 95°C for 2 min;
600 35 cycles of 95°C for 30 s, 60°C for 30 s, and 72°C for 30 s; 1 cycle of 72°C for 5 minutes.
601 Primer sequences for all reactions are listed in Table S4. We purified the PCR product using a
602 Monarch PCR & DNA cleanup kit (NEB #T1030). All samples were Sanger sequenced through
603 Azenta Life Sciences (South Plainfield, NJ, USA).
604
605 **Phenotyping and crossing**
606 To phenotype gonads, we euthanized adult stickleback fish at six- or twelve-months post
607 hatching in 0.05% MS-222 buffered to neutral. We dissected out the gonads and fixed one or
608 both gonads for 24 to 48 hours in 10% neutral buffered formalin. The remainder of the fish was
609 preserved in 75% ethanol. The gonads were processed, embedded in paraffin, sectioned at 5
610 µm, and stained with hematoxylin and eosin by the University of Georgia College of Veterinary

611 Medicine Histology Lab. We used a Zeiss Axio Scope A1 microscope and Zeiss Axiocam 305
612 Color camera to capture all images at the University of Georgia Biomedical Microscopy Core.
613 To make crosses, we euthanized mutant or wildtype male stickleback and gently
614 macerated testes in 500 µl of Hanks' Balanced Salt Solution. We stripped eggs from gravid
615 females and applied approximately 50 µl of sperm solution with a disposable transfer pipette.
616 We photographed adult stickleback with a Samsung Galaxy S22 under standardized lighting.
617
618 **Riboprobe synthesis**
619 We generated riboprobe templates for *gsdf, dmrt1, foxl2,* and *cyp10a1a* from cDNA from
620 adult gonads. We extracted total RNA from mature testis and ovary tissue using TRIzol Reagent
621 (Invitrogen 15596026) according to manufacturer's instructions. We synthesized cDNA using the
622 iScript cDNA Synthesis Kit (Bio-Rad 1708891) and amplified the targeted region for each gene
623 through PCR as described above (Table S4). We cloned the PCR product into plasmid pJC53.2
624 (kindly shared by Kendall Clay and Rachel Roberts-Galbraith) after digestion with Eam1105I
625 (Thermo Scientific FD0244) as in Collins *et al*. 2010 [143]. We verified each riboprobe template
626 after cloning with sanger sequencing by Azenta Life Sciences (South Plainfield, NJ, USA). For
627 *amha*, we ordered a synthetic gene fragment from TWIST Bioscience (San Francisco, CA, USA)
628 containing a 307 bp region of the *amha* cds flanked by a 5' T3 promoter and 3' T7 promoter to
629 facilitate riboprobe synthesis (File S2).
630 To synthesize riboprobes, we PCR amplified linear template from the appropriate
631 plasmid or used the synthetic gene fragment directly. We performed *in vitro* transcription from
632 these templates using T7 (New England Biolabs M0251S), T3 (New England Biolabs M0378S),
633 or SP6 (New England Biolabs M0207S) RNA polymerase according to manufacturer's
634 instructions, substituting 0.2 mM of UTP for DIG-labeled UTP (Roche 11209256910). We
635 purified riboprobes with a DNase treatment (New England Biolabs M0303S) and an ammonium
636 acetate precipitation.

637

638 ***In situ* hybridization**

639 We adapted a colorimetric *in situ* hybridization (ISH) protocol from Square, *et al.* 2021
640 [144]. We fixed the dissected gonads for 24-48 hours in 10% neutral buffered formalin. The
641 gonads were processed, embedded in paraffin, and sectioned at 5 µm by the University of
642 Georgia College of Veterinary Medicine Histology Lab. Unless otherwise stated, we performed
643 all steps in Lock-Mailer microscope slide jars in a volume of 9-11mL and at room temperature.
644 To deparaffinize, we warmed the slides in a 65°C incubator for five minutes, allowed them to
645 cool to room temperature, then washed the slides in Hemo-De once for 5 minutes then again for
646 10 minutes. We performed prehybridization washes indicated with an asterisk in a Tissue-Tek II
647 Slide Staining Station rather than Lock-Mailer jars: 100% EtOH for 5 minutes*, 80% EtOH for 10
648 minutes*, Milli-Q water for 10 minutes*, PBST for 5 minutes*, 15 ug/mL proteinase K in PBST
649 for 5 minutes, PBST rinse*, 4% PFA for 20 minutes, PBST twice for 10 minutes each*, 67°C pre-
650 heated hybridization buffer (50% formamide, 5X SSC, 0.1% Tween, 5mg/mL CHAPS, 0.1
651 mg/mL yeast RNA, 0.1mg/mL heparin, pH 6.0 with citric acid) twice for 5 minutes each, and pre-
652 heated hybridization buffer for 1 to 4 hours on a rotator at 67°C. We performed hybridization
653 with 100-500 ng/mL of riboprobe in hybridization buffer incubated overnight rotating at 67°C. We
654 stored hybridization solution at 20°C and reused up to 3 times.

655 Post-hybridization, we washed the slides 6 times with hybridization wash (50%
656 formamide, 5X SSC, 0.1% Tween) rotating at 67°C for 20-90 minutes each, totaling 5 to 6
657 hours. We rinsed the slides in MABT (maleic acid buffer with Tween) and washed them in MABT
658 for twice for 20 minutes each, first at 67°C, then at room temperature. We added blocking
659 solution (2% Blocking Reagent (Roche 11096176001) in MAB) to each slide, covered the slides
660 with parafilm, and incubated for 1 to 3 hours in a humidor. We poured off the blocking solution
661 and added 1:2000 anti-digoxigenin alkaline phosphate antibody (Roche 11093274910) in
662 blocking solution, covered the slides with parafilm, and left them in a humidor overnight at 4°C.

663 We performed five 20-50 minute post-antibody washes hybridization wash solution (50%
664 formamide, 5X SSC, 0.1% Tween, citric acid to pH 6.0) on a rotator for a total of three to four
665 hours, followed by an overnight MABT wash at 4°C.

666 Prior to coloration, we performed three 5-to-10-minute washes in NTMT (0.1 M NaCl, 0.1
667 M Tris pH 9.5, 0.05 M MgCl2, 0.1% Tween). We moved the slides into coloration solution
668 (blocking solution plus 25 ug/mL NBT and 175 ug/mL BCIP) and incubated 2 to 30 hours
669 covered to block light. We removed the slides from coloration solution once the color was stable
670 in the positive control (*gsdf*), but before any background color was seen in the negative control
671 (sense *gsdf*). Once coloration was complete, we rinsed the slides with PBST and washed for 10
672 minutes in PBST. We fixed the slides in 4% PFA in PBS at 4°C for one to five days.

673 To prepare slides for mounting, we performed three 5-minute washes in PBST and three
674 5-minute washes in deionized water. We mounted and coverslipped the slides using Vectashield
675 antifade mounting medium with DAPI. We used a Zeiss Axio Scope A1 microscope and Zeiss
676 Axiocam 305 Color camera to capture all images at the University of Georgia Biomedical
677 Microscopy Core.

678

679 **Sequence Alignments**

680 We retrieved sequences for *amha* (Gene ID: 120823390) and *amhy* (Gene ID:
681 120812167) from threespine assembly GAculeatus_UGA_version5 (GCF_016920845.1) and
682 *amh* (Gene ID: 119216504) from ninespine assembly fPunPun2.1 (GCA_949316345.1). We
683 performed all alignments and calculated sequence identity between *amh* homologues with
684 Muscle 5.1 [145] within Geneious Prime (v2024.0.5) using default parameters. We defined
685 intron and exon positions based upon the threespine *amha* sequence in each alignment. We
686 calculated dN/dS with the R package ape v5.8-1 [146] using the translation aligned coding
687 sequences of *amha* (XM_040183306.1), *amhy* (XM_040167960.1), and ninespine *amh*
688 (XM_037469420.2). One additional base was included at the 5' end of exon 7 of the ninespine

689 *amh* cds in order to correct the predicted annotation which contains multiple premature stop
690 codons in this final exon. Alignment files are presented in File S2. We generated Vistaplots
691 [147,148] using LAGAN [149] alignments and a 100 bp window size with a 70% sequence
692 identity threshold.
693
694 **RNAseq**
695 We staged embryos according to established stickleback developmental stages [79] and
696 preserved the whole embryos in RNAlater Stabilization Solution (Invitrogen AM7021) following
697 manufacturer guidelines and stored at -80 °C until analysis. We extracted RNA using TRIzol
698 Reagent (Invitrogen 15596026) and the Direct-zol RNA Microprep Kit (Zymo R2062). We
699 created sequencing libraries using the Illumina TruSeq Stranded mRNA Library Prep kit
700 (20020594). We pooled the libraries from all samples and 150 bp paired end reads were
701 sequenced on two lanes using a NovaSeq X Plus by Azenta Life Sciences (South Plainfield, NJ,
702 USA). All of the samples were sequenced to an average of 34.7 M read depth (min 11.6 M, max
703 71.3 M, SD = 10.4 M) (File S1). We trimmed raw reads for quality and sequencing adapters with
704 Trimmomatic (v. 0.39) [150] using leading and trailing quality threshold of 3, a sliding window of
705 4 with quality threshold of 15, and minimum length cutoff of 36. We aligned paired and orphan
706 reads to the threespine stickleback reference genome (GAculeatus_UGA_version5, NCBI
707 RefSeq assembly GCF_016920845.1) using HISAT-3N [151] with default parameters. All
708 samples had an alignment rate between 73% and 92% (File S1). We generated Indexed BAM
709 files of the alignments with Samtools (v. 1.17). We generated transcript counts against the NCBI
710 annotation GTF file (release 100) for GCF_016920845.1 with HTseq (v. 2.0.2) [152] using
711 HTSeq-count with default parameters except --stranded=no. We performed all remaining
712 analyses in R (v. 4.4.1) and RStudio (v. 2024.04.2+764). We combined the counts from paired
713 and orphaned reads for each sample and used DESeq2 (v. 1.44.0) [153] to generate normalized
714 read counts and perform differential expression analysis. We identified DEGs using the standard

workflow with stage and sex combined as a single factor. We used the contrast function to calculate log2 fold changes (logFC) and adjusted p values for differential expression between males and females at each timepoint. We identified DEGs of interest using GO terms from the NIH gene2go database (https://ftp.ncbi.nlm.nih.gov/gene/DATA/).

Material Availability

RNAseq data is available in the short reads archive under BioProject PRJNA1248589. All scripts are available at https://github.com/MTreasterUGA/Amhy-sex-determination. All plasmids are available upon request.

Acknowledgements

This work was funded by the National Science Foundation MCB 1943283 (M.A.W), the National Institutes of Health 1T32GM142623 (M.J.T.), The University of Georgia Research Foundation (M.J.T.), the Society for the Study of Evolution R.C. Lewontin Early Award (M.J.T.), and ARCS foundation (M.J.T.).

Research reported in this publication was supported by the National Institute of General Medical Sciences of the National Institutes of Health under Award Number R01GM147312 (M.A.W). The content is solely the responsibility of the authors and does not necessarily represent the official views of the National Institutes of Health.

This study was supported in part by resources and technical expertise from the Georgia Advanced Computing Resource Center, a partnership between the University of Georgia's Office of the Vice President for Research and Office of the Vice President for Information Technology.

The imaging data used in this publication was produced in collaboration with the Biomedical Microscopy Core at the University of Georgia.

We thank Koichi Kawakami (National Institute of Genetics, Japan) for use of the Tol2 elements in this study.

Declaration of Interests

The authors declare no conflicts of interests

746 **Figures and tables**

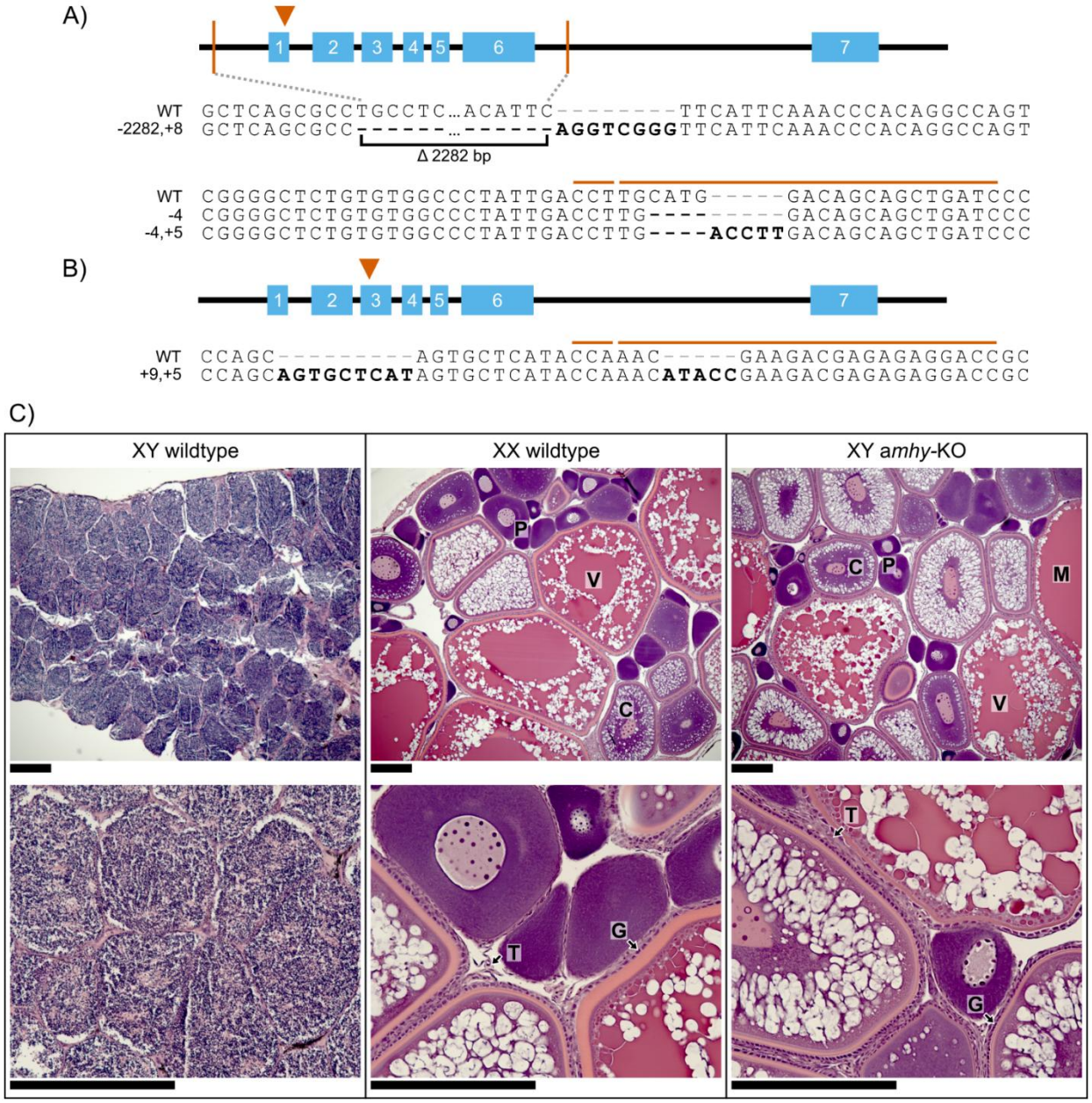

747

748 Fig 1. CRISPR/Cas9 knockout of *amhy* caused male to female sex reversal in F1 XY fish.

749 We used CRISPR/Cas9 to target exon 1 (A) or exon 2 (B) of *amhy*. CRISPR target site and

750 PAM sequence are indicated by orange lines above wildtype reference sequence. Mutations

751 relative to wildtype are bolded. We identified four loss of function *amhy* alleles in F1 progeny.

752 One allele (-2282,+8) deleted the first six exons of *amhy*. Other alleles featured small frameshift

753 indels. C) We identified male to female sex reversal using gonad morphology and histology.
754 Ovaries in XX wildtype and XY *amhy*-KO fish feature oocytes throughout multiple stages of
755 development. P – primary oocyte, C – cortical alveolus stage V – vitellogenic stage, M – Mature
756 oocyte, G – Granulosa cells, T – Theca cells. Scale bars = 200 µm.
757

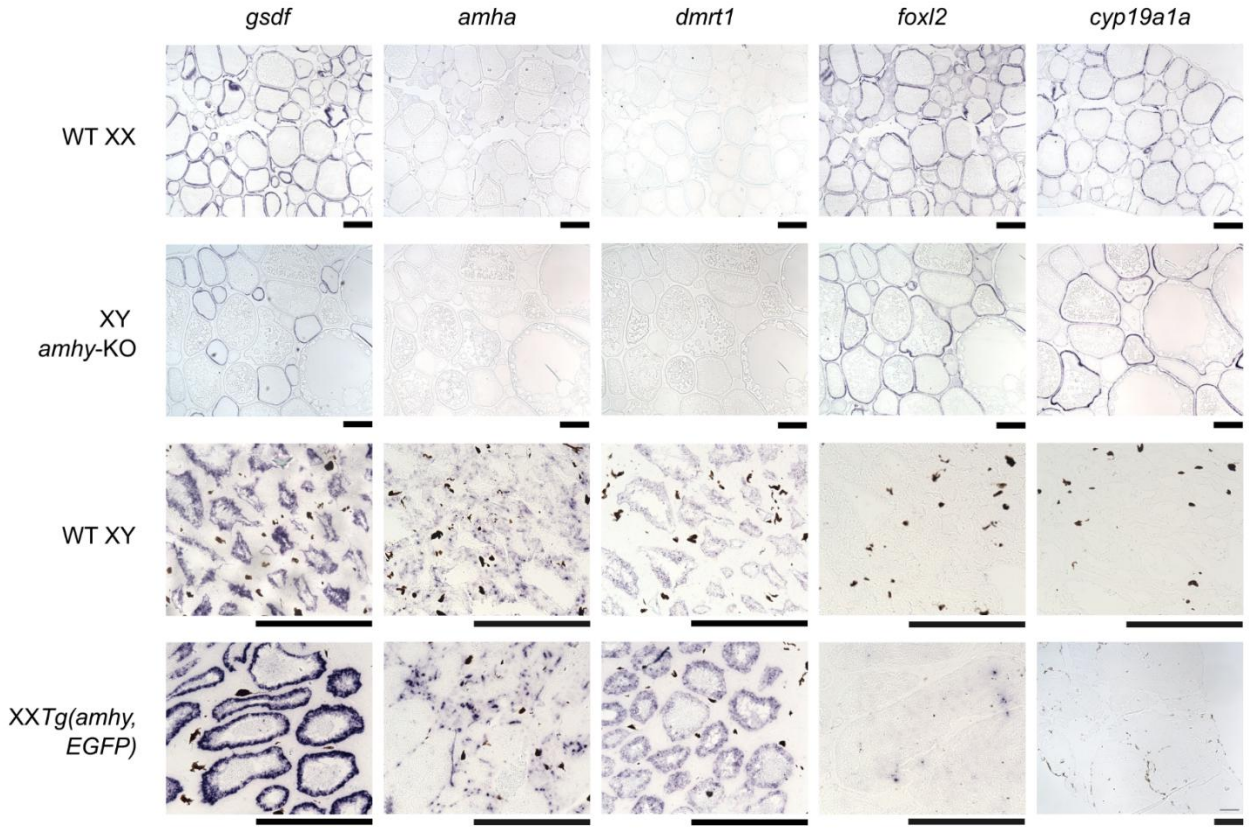

758
759 Fig 2. Gene expression in sex reversed gonads resembles expression in wild type gonads.
760 *In situ* hybridization of gonadal genes in wildtype and sex reversed stickleback gonads. A
761 positive control gene *gsdf* was expressed in somatic cells of both testes and ovaries. Wildtype
762 XY and sex reversed XX testes show strong expression of male differentiation genes *amha* and
763 *dmrt1* but not female differentiaiton genes *foxl2* and *cyp19a1a*. Wildtype XX and sex reversed
764 XY ovaries strongly express female differentiation genes but not male differentiation genes.
765 Scale bars = 200 µm.
766

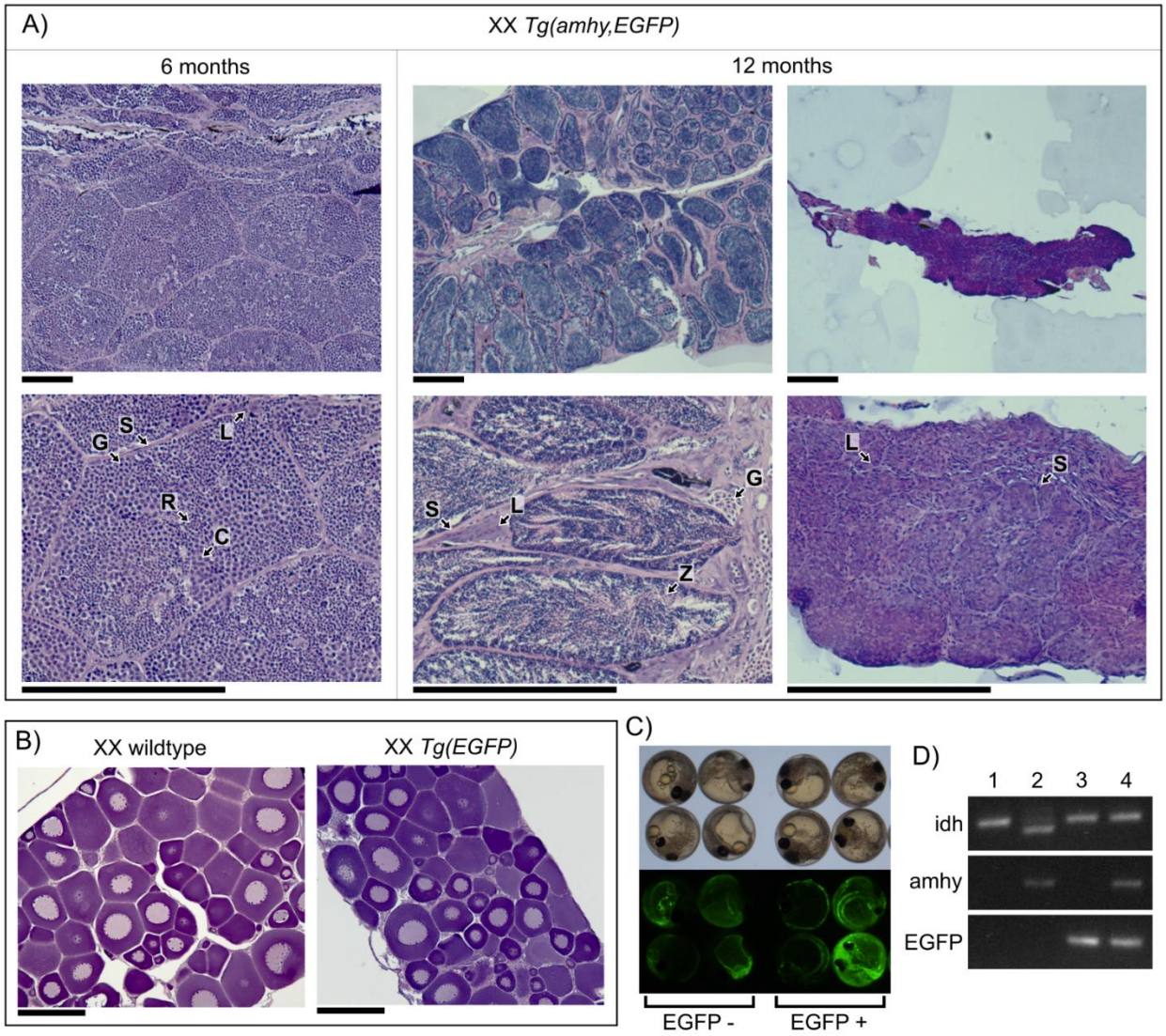

767

768 Fig 3. XX fish with an *amhy* transgene exhibit female to male sex reversal.

769 A) XX *Tg(-5amhy3.5,Xla.Ef1a:EGFP)* fish developed testes with varying cell composition. At 12
770 months post hatching, fish had either normal testes with mature sperm (middle) or hypotrophic
771 testes without discernable germ cells (right). G – spermatogonia, C – spermatocyte, R – round
772 spermatid, Z – Spermatozoa, L – Leydig cells, S – Sertoli cells Scale bars = 200 μm. B) Control
773 XX *Tg(Xla.Ef1a:EGFP)* fish developed ovaries identical to wildtype XX counterparts. Scale bars
774 = 200 μm. C) Embryos injected with pT2-5amhy3.5,Xla.Ef1a:EGFP seven days after fertilization
775 under bright field (top) and EGFP excitation (bottom). Embryos positive for transgene integration
776 show somatic EGFP expression. We removed embryos with no EGFP expression or EGFP

expression only in the yolk, which indicates the yolk was injected rather than the blastomere [40]. D) We used PCR of the sex-linked marker *idh* to genotype XX and XY fish. PCR of EGFP and *amhy* show the presence of the associated transgene. 1 – wildtype XX, 2 – wildtype XY, 3 – XX *Tg(EGFP)*, 4 – XX *Tg(amhy,EGFP)*.

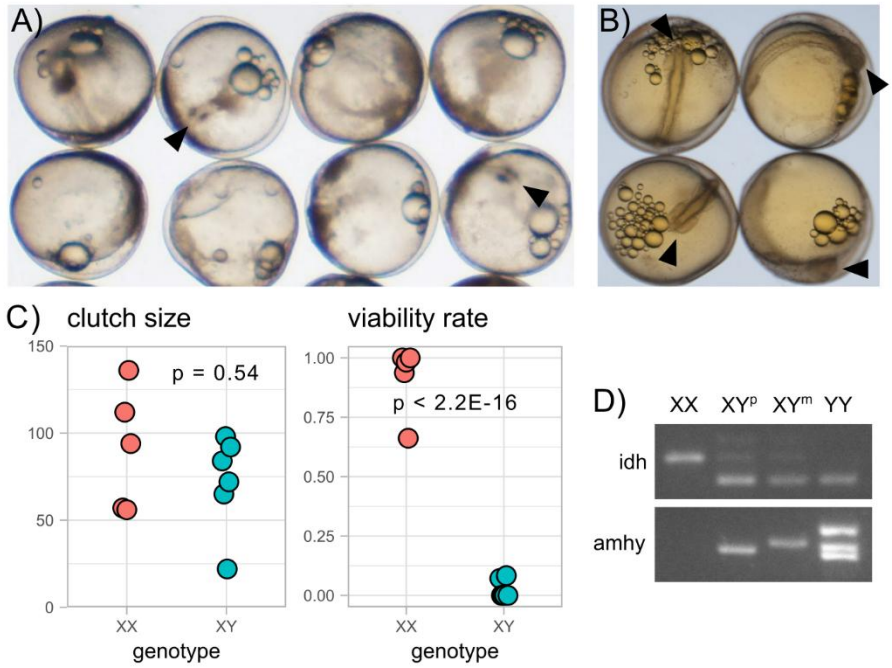

Fig 4. XY *amhy*-KO females can reproduce and transmit an X or Y chromosome. YY embryos (A) at 48 hours post fertilization show arrested development compared to wildtype embryos (B). Arrowheads denote anterior end of body axis. C) F2 XX and XY *amhy*-KO female siblings do not show a significant difference in clutch size (wilcoxon test, $p < 0.05$). Clutches from XY *amhy*-KO females have a significantly lower viability rate than those from XX female siblings (z test, $p < 0.05$). D) PCR of the sex linked marker IDH shows the absence of the X chromosome in YY embryos. Both the paternal (wildtype) and maternal (+9,+5) loss of function alleles can be detected in XY offspring. YY embryos show the presence of both amhy alleles as well as a third band, likely a heterodimer of the maternal and paternal amplicons.

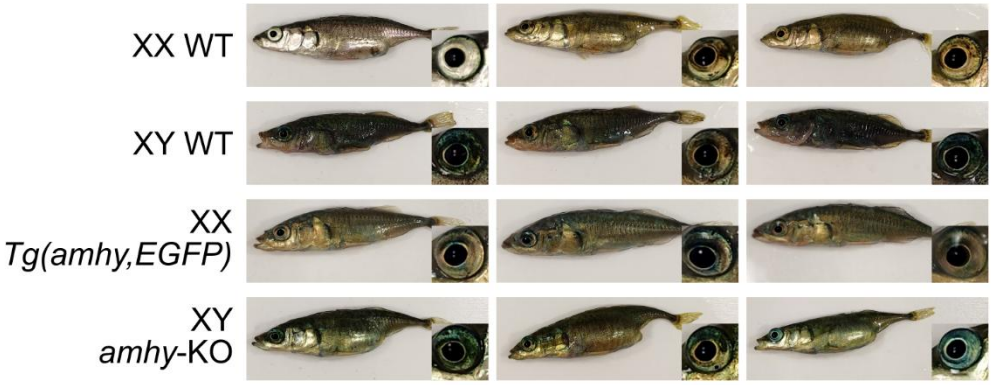

Fig 5. Both male and female sex reversed stickleback show partial male nuptial coloration. Wildtype and mutant threespine stickleback at one year post hatching. Wildtype XX females are silver and may darken slightly when gravid. Wildtype XY males have dark blue eyes and bodies and red throats. Sex reversed XX *Tg(amhy,EGFP)* males are less dark than wildtype males but show blue coloration on the body and eyes. Sex reversed XY *amhy*-KO females show slight or moderate darkening of the body with distinct blue eyes not typical of wildtype XX females.

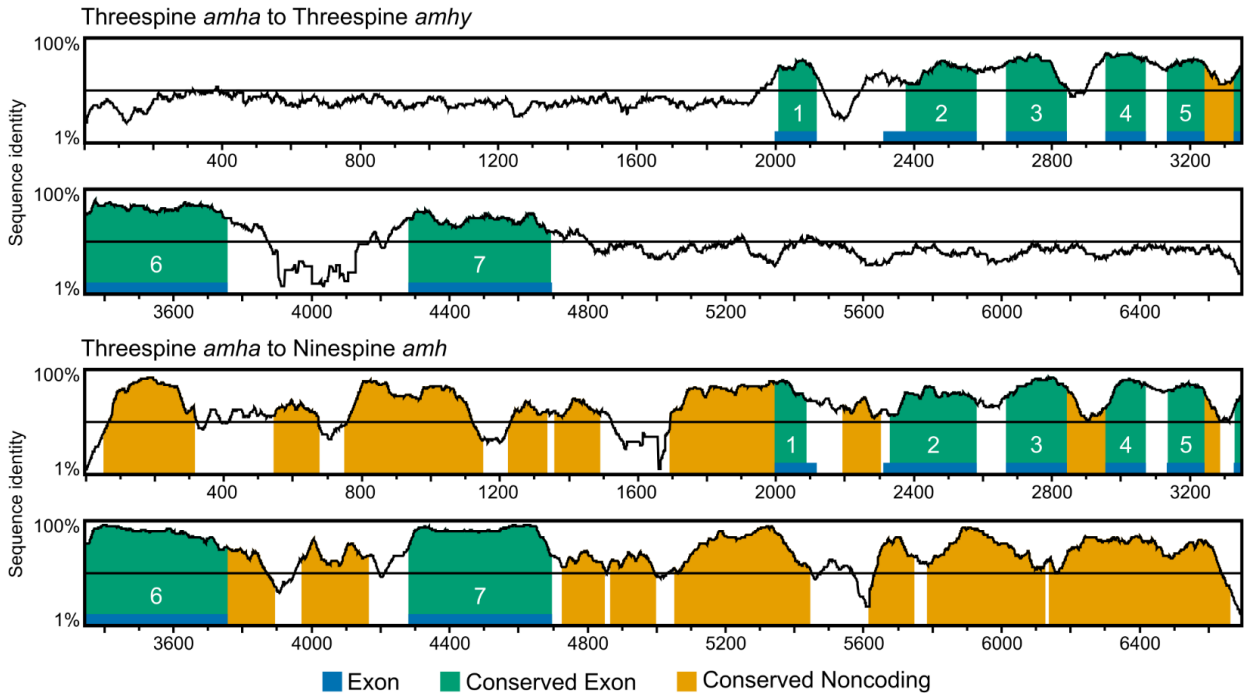

Fig 6. *amha* and *amhy* show no sequence conservation outside of the coding sequence. Vistaplots showing conserved sequence identity of threespine *amha* to threespine *amhy* (top) and to ninespine *amh* (bottom) with sequence identity on the y axis and nucleotide position of threespine *amha* on the x axis. Exon positions are indicated along the x axis in blue. Conserved exon and noncoding sequences share 70% sequence identity in a 100 bp window.

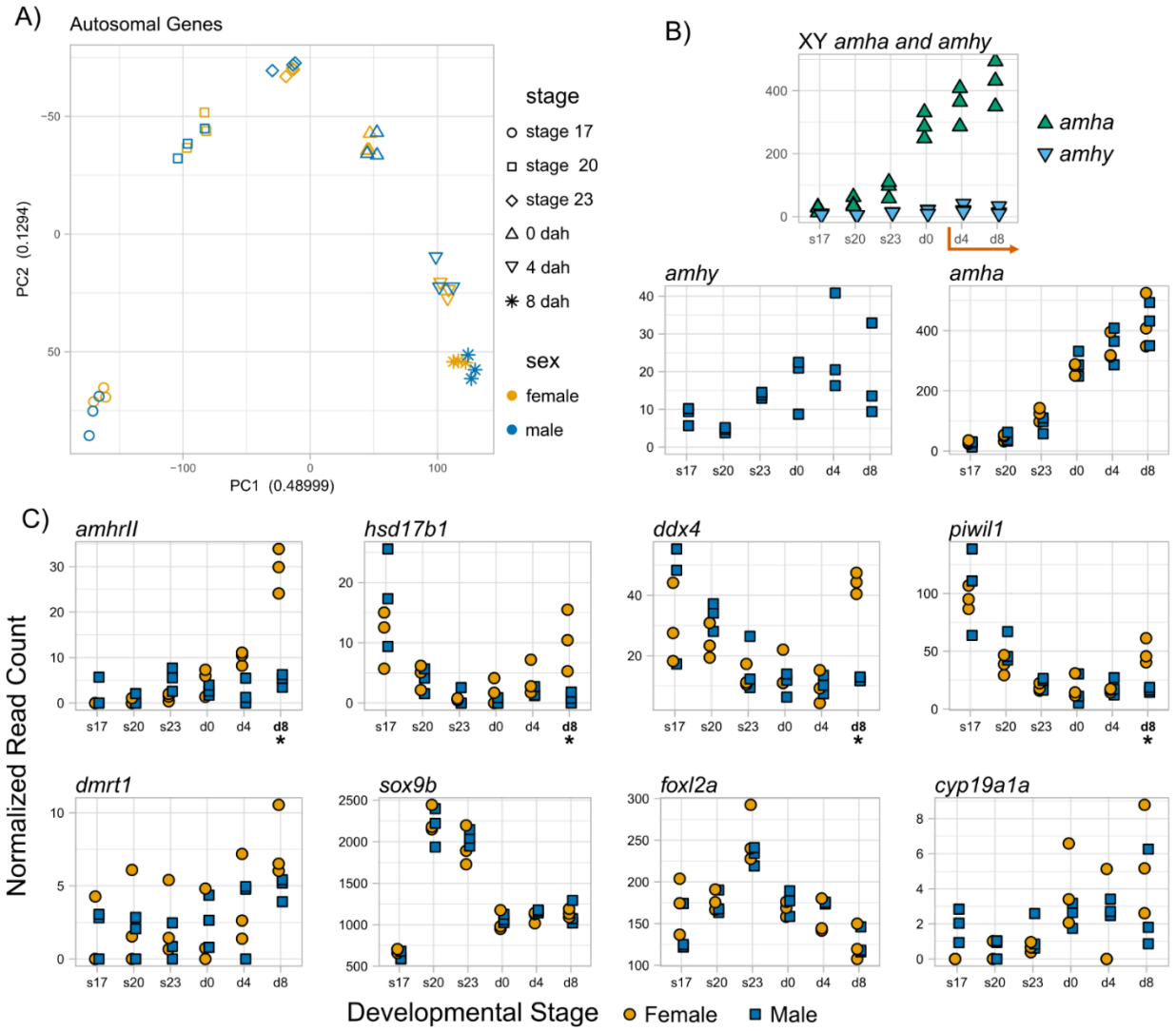

Fig 7. Expression of gonadal growth and differentiation genes in embryonic and larval stickleback.

(A) PCA plots of normalized read counts for all genes cluster by stage rather than sex. (B) and (C) Normalized read counts of genes in embryonic stages 17, 20, 23, and larvae 0, 4, and 8 days after hatching. Stages with significant differences between males and females are marked with an asterisk and bolded (Benjamini Hochberg adjusted p value < 0.05; Table 2). The orange arrow (B) indicates stages where differences in germ counts have been observed between males and females.

818 Table 1. Sequence conservation of the threespine *amha* to threespine *amhy* and ninespine *amh.*

Threespine *amha* and threespine *amhy*											
	Exon 1	Exon 2	Exon 3	Exon 4	Exon 5	Exon 6	Exon 7	CDS	Introns	2kb Upstream	2kb Downstream
Sequence identity	0.760	0.682	0.812	0.866	0.790	0.846	0.742	0.780	0.286	0.365	0.376
dN/dS	0.583	0.362	0.512	0.803	0.651	0.373	0.723	0.534	-	-	-
Threespine *amha* and ninespine *amh*											
	Exon 1	Exon 2	Exon 3	Exon 4	Exon 5	Exon 6	Exon 7	CDS	Introns	2kb Upstream	2kb Downstream
Sequence identity	0.791	0.769	0.890	0.920	0.870	0.905	0.936	0.879	0.668	0.595	0.660
dN/dS	0.597	0.425	1.003	0.441	0.266	0.565	0.278	0.467	-	-	-

819

820

821 Table 2. Benjamini Hochberg adjusted P values for differential expression between males and

822 females.

gene	gene id	stage 17	stage 20	stage 23	0 dah	4 dah	8 dah
amha	amh	1	1	0.679	1	1	1
amhrII	LOC120835457	0.952	1	0.322	1	0.509	**0.0280**
ddx4	ddx4	1	1	1	1	1	**0.00193**
piwil1	piwil1	1	1	1	1	1	**0.00403**
hsd17b1	hsd17b1	1	1	1	0.8681	1	**0.0238**
foxl2a	foxl2a	0.788	1	1	1	1	1
cyp19a1a	LOC120811580	0.662	1	1	1	1	1
dmrt1	dmrt1	1	1	1	1	1	1
sox9b	LOC120827768	0.930	1	1	1	1	1
gsdf	gsdf	1	1	0.467	1	1	1
nr5a1	nr5a1a	1	1	1	1	1	0.983

823

824

825 Table 3. Phenotypes of mutant stickleback from this study

Genotype	**N**	**Male (%)**	**Female (%)**
F0 XY *amhy* crispants	17	9 (53%)	8 (47%)
F1 XY *amhy*-KO	16	0 (0%)	16 (100%)
F0 XX *Tg(-5amhy2.5,Xla.Ef1a:EGFP)*	16	16 (100%)	0 (0%)
F0 XX *Tg(Xla.Ef1a:EGFP)*	10	0 (0%)	10 (100%)

826

827

828 **References**

829 1. Bachtrog D, Mank JE, Peichel CL, Kirkpatrick M, Otto SP, Ashman T-L, et al. Sex
830 Determination: Why So Many Ways of Doing It? PLoS Biol. 2014;12: e1001899.
831 doi:10.1371/journal.pbio.1001899

832 2. Capel B. Vertebrate sex determination: evolutionary plasticity of a fundamental switch.
833 Nat Rev Genet. 2017;18: 675–689. doi:10.1038/nrg.2017.60

834 3. Weber C, Capel B. Sex determination without sex chromosomes. Philosophical
835 Transactions of the Royal Society B: Biological Sciences. 2021;376: 20200109.
836 doi:10.1098/rstb.2020.0109

837 4. Charlesworth D, Charlesworth B, Marais G. Steps in the evolution of heteromorphic sex
838 chromosomes. Heredity. 2005;95: 118–128. doi:10.1038/sj.hdy.6800697

839 5. Charlesworth B, Charlesworth D. A Model for the Evolution of Dioecy and Gynodioecy.
840 The American Naturalist. 1978;112: 975–997. doi:10.1086/283342

841 6. Ponnikas S, Sigeman H, Abbott JK, Hansson B. Why Do Sex Chromosomes Stop
842 Recombining? Trends in Genetics. 2018;34: 492–503. doi:10.1016/j.tig.2018.04.001

843 7. Pan Q, Kay T, Depincé A, Adolfi M, Schartl M, Guiguen Y, et al. Evolution of master sex
844 determiners: TGF-β signalling pathways at regulatory crossroads. Philosophical
845 Transactions of the Royal Society B: Biological Sciences. 2021;376: 20200091.
846 doi:10.1098/rstb.2020.0091

847 8. Takehana Y, Matsuda M, Myosho T, Suster ML, Kawakami K, Shin-I T, et al. Co-option of
848 Sox3 as the male-determining factor on the Y chromosome in the fish Oryzias dancena.
849 Nat Commun. 2014;5: 4157. doi:10.1038/ncomms5157

850 9. Shan Z, Nanda I, Wang Y, Schmid M, Vortkamp A, Haaf T. Sex-specific expression of an
851 evolutionarily conserved male regulatory gene, DMRT1, in birds. Cytogenetics and Cell
852 Genetics. 2000;89: 252–257. doi:10.1159/000015626

853 10. Yoshimoto S, Okada E, Umemoto H, Tamura K, Uno Y, Nishida-Umehara C, et al. A W-
854 linked DM-domain gene, DM-W, participates in primary ovary development in Xenopus
855 laevis. Proceedings of the National Academy of Sciences. 2008;105: 2469–2474.
856 doi:10.1073/pnas.0712244105

857 11. Matsuda M, Nagahama Y, Shinomiya A, Sato T, Matsuda C, Kobayashi T, et al. DMY is a
858 Y-specific DM-domain gene required for male development in the medaka fish. Nature.
859 2002;417: 559–563. doi:10.1038/nature751

860 12. Nanda I, Kondo M, Hornung U, Asakawa S, Winkler C, Shimizu A, et al. A duplicated copy
861 of DMRT1 in the sex-determining region of the Y chromosome of the medaka, Oryzias

latipes. Proceedings of the National Academy of Sciences. 2002;99: 11778–11783. doi:10.1073/pnas.182314699

13. Hattori RS, Murai Y, Oura M, Masuda S, Majhi SK, Sakamoto T, et al. A Y-linked anti-Mullerian hormone duplication takes over a critical role in sex determination. Proceedings of the National Academy of Sciences. 2012;109: 2955–2959. doi:10.1073/pnas.1018392109

14. Hattori RS, Somoza GM, Fernandino JI, Colautti DC, Miyoshi K, Gong Z, et al. The Duplicated Y-specific amhy Gene Is Conserved and Linked to Maleness in Silversides of the Genus Odontesthes. Genes. 2019;10: 679. doi:10.3390/genes10090679

15. Hattori RS, Kumazawa K, Nakamoto M, Nakano Y, Yamaguchi T, Kitano T, et al. Y-specific amh allele, amhy, is the master sex-determining gene in Japanese flounder Paralichthys olivaceus. Frontiers in Genetics. 2022;13. Available: https://www.frontiersin.org/articles/10.3389/fgene.2022.1007548

16. Li M, Sun Y, Zhao J, Shi H, Zeng S, Ye K, et al. A Tandem Duplicate of Anti-Müllerian Hormone with a Missense SNP on the Y Chromosome Is Essential for Male Sex Determination in Nile Tilapia, Oreochromis niloticus. Naruse K, editor. PLoS Genet. 2015;11: e1005678. doi:10.1371/journal.pgen.1005678

17. Rondeau EB, Laurie CV, Johnson SC, Koop BF. A PCR assay detects a male-specific duplicated copy of Anti-Müllerian hormone (amh) in the lingcod (Ophiodon elongatus). BMC Research Notes. 2016;9: 230. doi:10.1186/s13104-016-2030-6

18. Bej DK, Miyoshi K, Hattori RS, Strüssmann CA, Yamamoto Y. A Duplicated, Truncated amh Gene Is Involved in Male Sex Determination in an Old World Silverside. G3 Genes|Genomes|Genetics. 2017;7: 2489–2495. doi:10.1534/g3.117.042697

19. Pan Q, Feron R, Yano A, Guyomard R, Jouanno E, Vigouroux E, et al. Identification of the master sex determining gene in Northern pike (Esox lucius) reveals restricted sex chromosome differentiation. PLOS Genetics. 2019;15: e1008013. doi:10.1371/journal.pgen.1008013

20. Peichel CL, McCann SR, Ross JA, Naftaly AFS, Urton JR, Cech JN, et al. Assembly of the threespine stickleback Y chromosome reveals convergent signatures of sex chromosome evolution. Genome Biol. 2020;21: 177. doi:10.1186/s13059-020-02097-x

21. Song W, Xie Y, Sun M, Li X, Fitzpatrick CK, Vaux F, et al. A duplicated amh is the master sex-determining gene for Sebastes rockfish in the Northwest Pacific. Open Biology. 2021;11: 210063. doi:10.1098/rsob.210063

22. Jeffries DL, Mee JA, Peichel CL. Identification of a candidate sex determination gene in Culaea inconstans suggests convergent recruitment of an Amh duplicate in two lineages of stickleback. Journal of Evolutionary Biology. 2022;n/a. doi:10.1111/jeb.14034

23. Zhao H, Li J, Xiao Z, Xiao Y. Dose-dependent role of AMH and AMHR2 signaling in male differentiation and regulation of sex determination in Spotted knifejaw (Oplegnathus punctatus) with X1X1X2X2/X1X2Y chromosome system. Cell Communication and Signaling. 2025;23: 59. doi:10.1186/s12964-025-02038-w

24. Cortez D, Marin R, Toledo-Flores D, Froidevaux L, Liechti A, Waters PD, et al. Origins and functional evolution of Y chromosomes across mammals. Nature. 2014;508: 488–493. doi:10.1038/nature13151

25. Mullen RD, Ontiveros AE, Moses MM, Behringer RR. AMH and AMHR2 mutations: A spectrum of reproductive phenotypes across vertebrate species. Developmental Biology. 2019;455: 1–9. doi:10.1016/j.ydbio.2019.07.006

26. Howard JA, Hart KN, Thompson TB. Molecular Mechanisms of AMH Signaling. Frontiers in Endocrinology. 2022;13. Available: https://www.frontiersin.org/articles/10.3389/fendo.2022.927824

27. Baarends WM, Helmond MJL van, Post M, Schoot PJCM van der, Hoogerbrugge JW, Winter JP de, et al. A novel member of the transmembrane serine/threonine kinase receptor family is specifically expressed in the gonads and in mesenchymal cells adjacent to the müllerian duct. Development. 1994;120: 189–197. doi:10.1242/dev.120.1.189

28. Josso N, di Clemente N, Gouédard L. Anti-Müllerian hormone and its receptors. Molecular and Cellular Endocrinology. 2001;179: 25–32. doi:10.1016/S0303-7207(01)00467-1

29. Mishina Y, Whitworth DJ, Racine C, Behringer RR. High Specificity of Müllerian-Inhibiting Substance Signaling in Vivo*. Endocrinology. 1999;140: 2084–2088. doi:10.1210/endo.140.5.6705

30. Jost A. The Age Factor in the Castration of Male Rabbit Fetuses. Proceedings of the Society for Experimental Biology and Medicine. 1947;66: 302–303. doi:10.3181/00379727-66-16071

31. Morinaga C, Saito D, Nakamura S, Sasaki T, Asakawa S, Shimizu N, et al. The hotei mutation of medaka in the anti-Müllerian hormone receptor causes the dysregulation of germ cell and sexual development. PNAS. 2007;104: 9691–9696. doi:10.1073/pnas.0611379104

32. Pfennig F, Standke A, Gutzeit HO. The role of Amh signaling in teleost fish – Multiple functions not restricted to the gonads. General and Comparative Endocrinology. 2015;223: 87–107. doi:10.1016/j.ygcen.2015.09.025

33. Yan Y-L, Batzel P, Titus T, Sydes J, Desvignes T, BreMiller R, et al. A Hormone That Lost Its Receptor: Anti-Müllerian Hormone (AMH) in Zebrafish Gonad Development and Sex Determination. Genetics. 2019;213: 529–553. doi:10.1534/genetics.119.302365

34. Ross JA, Urton JR, Boland J, Shapiro MD, Peichel CL. Turnover of Sex Chromosomes in the Stickleback Fishes (Gasterosteidae). PLOS Genetics. 2009;5: e1000391. doi:10.1371/journal.pgen.1000391

35. Dixon G, Kitano J, Kirkpatrick M. The Origin of a New Sex Chromosome by Introgression between Two Stickleback Fishes. Molecular Biology and Evolution. 2019;36: 28–38. doi:10.1093/molbev/msy181

36. Natri HM, Merilä J, Shikano T. The evolution of sex determination associated with a chromosomal inversion. Nat Commun. 2019;10: 145. doi:10.1038/s41467-018-08014-y

37. Sardell JM, Josephson MP, Dalziel AC, Peichel CL, Kirkpatrick M. Heterogeneous Histories of Recombination Suppression on Stickleback Sex Chromosomes. Molecular Biology and Evolution. 2021;38: 4403–4418. doi:10.1093/molbev/msab179

38. Peichel CL, Ross JA, Matson CK, Dickson M, Grimwood J, Schmutz J, et al. The Master Sex-Determination Locus in Threespine Sticklebacks Is on a Nascent Y Chromosome. Current Biology. 2004;14: 1416–1424. doi:10.1016/j.cub.2004.08.030

39. Pigott GC, Akel MA, Rogers MGQ, Flanagan ME, Marlette EG, Treaster MJ, et al. Evidence for Variation in the Genetic Basis of Sex Determination in Brook Stickleback (Culaea inconstans). Ecology and Evolution. 2025;15: e70955. doi:10.1002/ece3.70955

40. Erickson PA, Ellis NA, Miller CT. Microinjection for Transgenesis and Genome Editing in Threespine Sticklebacks. J Vis Exp. 2016 [cited 30 Jan 2021]. doi:10.3791/54055

41. Nath S, Shaw DE, White MA. Improved contiguity of the threespine stickleback genome using long-read sequencing. G3 Genes|Genomes|Genetics. 2021;11. doi:10.1093/g3journal/jkab007

42. Aguirre WE, Ellis KE, Kusenda M, Bell MA. Phenotypic variation and sexual dimorphism in anadromous threespine stickleback: implications for postglacial adaptive radiation. Biological Journal of the Linnean Society. 2008;95: 465–478. doi:10.1111/j.1095-8312.2008.01075.x

43. Leinonen T, Cano JM, Merilä J. Genetic basis of sexual dimorphism in the threespine stickleback Gasterosteus aculeatus. Heredity. 2011;106: 218–227. doi:10.1038/hdy.2010.104

44. Kitano J, Mori S, Peichel CL. Sexual Dimorphism in the External Morphology of the Threespine Stickleback (Gasterosteus Aculeatus). Copeia. 2007;2007: 336–349. doi:10.1643/0045-8511(2007)7[336:SDITEM]2.0.CO;2

45. Aguirre WE, Akinpelu O. Sexual dimorphism of head morphology in three-spined stickleback Gasterosteus aculeatus. Journal of Fish Biology. 2010;77: 802–821. doi:10.1111/j.1095-8649.2010.02705.x

46. Toli EA, Noreikiene K, DeFaveri J, Merilä J. Environmental enrichment, sexual dimorphism, and brain size in sticklebacks. Ecology and Evolution. 2017;7: 1691–1698. doi:10.1002/ece3.2717

47. Kotrschal A, Räsänen K, Kristjánsson BK, Senn M, Kolm N. Extreme Sexual Brain Size Dimorphism in Sticklebacks: A Consequence of the Cognitive Challenges of Sex and Parenting? PLOS ONE. 2012;7: e30055. doi:10.1371/journal.pone.0030055

48. McGee MD, Wainwright PC. Sexual dimorphism in the feeding mechanism of threespine stickleback. Journal of Experimental Biology. 2013;216: 835–840. doi:10.1242/jeb.074948

49. Whoriskey FG, FitzGerald GJ. Sex, cannibalism and sticklebacks. Behav Ecol Sociobiol. 1985;18: 15–18. doi:10.1007/BF00299233

50. King AJ, Fürtbauer I, Mamuneas D, James C, Manica A. Sex-Differences and Temporal Consistency in Stickleback Fish Boldness. PLOS ONE. 2013;8: e81116. doi:10.1371/journal.pone.0081116

51. FitzGerald GJ. The Reproductive Behavior of the Stickleback. Scientific American. 1993;268: 80–85.

52. Bell MA, Foster SA. The Evolutionary Biology of the Threespine Stickleback. The Journal of Animal Ecology. 1994;64: 418. doi:10.2307/5902

53. Pressley PH. Parental Effort and the Evolution of Nest-Guarding Tactics in the Threespine Stickleback, Gasterosteus aculeatus L. Evolution. 1981;35: 282–295. doi:10.2307/2407838

54. Bakker TCM, Künzler R, Mazzi D. Condition-related mate choice in sticklebacks. Nature. 1999;401: 234–234. doi:10.1038/45727

55. Milinski M, Bakker TCM. Female sticklebacks use male coloration in mate choice and hence avoid parasitized males. Nature. 1990;344: 330–333. doi:10.1038/344330a0

56. Conte GL, Schluter D. Experimental Confirmation That Body Size Determines Mate Preference via Phenotype Matching in a Stickleback Species Pair. Evolution. 2013;67: 1477–1484. doi:10.1111/evo.12041

57. Andreou D, Eizaguirre C, Boehm T, Milinski M. Mate choice in sticklebacks reveals that immunogenes can drive ecological speciation. Behavioral Ecology. 2017;28: 953–961. doi:10.1093/beheco/arx074

58. Milinski M. The function of mate choice in sticklebacks: optimizing Mhc genetics. Journal of Fish Biology. 2003;63: 1–16. doi:10.1111/j.1095-8649.2003.00215.x

59. Flamarique IN, Bergstrom C, Cheng CL, Reimchen TE. Role of the iridescent eye in stickleback female mate choice. Journal of Experimental Biology. 2013;216: 2806–2812. doi:10.1242/jeb.084889

60. Barker TCM, Milinski M. The advantages of being red: Sexual selection in the stickleback. Marine & Freshwater Behaviour & Phy. 1993 [cited 21 Apr 2025]. doi:10.1080/10236249309378870

61. Candolin U. Reproduction under predation risk and the trade–off between current and future reproduction in the threespine stickleback. Proceedings of the Royal Society of London Series B: Biological Sciences. 1998;265: 1171–1175. doi:10.1098/rspb.1998.0415

62. Johnson S, Candolin U. Predation cost of a sexual signal in the threespine stickleback. Behavioral Ecology. 2017;28: 1160–1165. doi:10.1093/beheco/arx080

1013 63. Borg B, Mayer I, Hoffmann E, Österman A. 11-ketotestosterone is not responsible for the
1014 entire testicular effect on male reproductive behaviour in the threespine stickleback.
1015 Behav. 2008;145: 509–525. doi:10.1163/156853908792451548

1016 64. Shibata Y, Paul-Prasanth B, Suzuki A, Usami T, Nakamoto M, Matsuda M, et al.
1017 Expression of gonadal soma derived factor (GSDF) is spatially and temporally correlated
1018 with early testicular differentiation in medaka. Gene Expression Patterns. 2010;10: 283–
1019 289. doi:10.1016/j.gep.2010.06.005

1020 65. Guo Y, Cheng H, Huang X, Gao S, Yu H, Zhou R. Gene structure, multiple alternative
1021 splicing, and expression in gonads of zebrafish *Dmrt1*. Biochemical and Biophysical
1022 Research Communications. 2005;330: 950–957. doi:10.1016/j.bbrc.2005.03.066

1023 66. von Hofsten J, Larsson A, Olsson P e. Novel steroidogenic factor-1 homolog (ff1d) is
1024 coexpressed with anti-Mullerian hormone (AMH) in zebrafish. Developmental Dynamics.
1025 2005;233: 595–604. doi:10.1002/dvdy.20335

1026 67. Johnsen H, Seppola M, Torgersen JS, Delghandi M, Andersen Ø. Sexually dimorphic
1027 expression of *dmrt1* in immature and mature Atlantic cod (*Gadus morhua* L.).
1028 Comparative Biochemistry and Physiology Part B: Biochemistry and Molecular Biology.
1029 2010;156: 197–205. doi:10.1016/j.cbpb.2010.03.009

1030 68. von Schalburg KR, Gowen BE, Rondeau EB, Johnson NW, Minkley DR, Leong JS, et al.
1031 Sex-specific expression, synthesis and localization of aromatase regulators in one-year-
1032 old Atlantic salmon ovaries and testes. Comparative Biochemistry and Physiology Part B:
1033 Biochemistry and Molecular Biology. 2013;164: 236–246. doi:10.1016/j.cbpb.2013.01.004

1034 69. Kossack ME, Draper BW. Genetic regulation of sex determination and maintenance in
1035 zebrafish (Danio rerio). Curr Top Dev Biol. 2019;134: 119–149.
1036 doi:10.1016/bs.ctdb.2019.02.004

1037 70. Urasaki A, Morvan G, Kawakami K. Functional Dissection of the Tol2 Transposable
1038 Element Identified the Minimal cis-Sequence and a Highly Repetitive Sequence in the
1039 Subterminal Region Essential for Transposition. Genetics. 2006;174: 639–649.
1040 doi:10.1534/genetics.106.060244

1041 71. Kawakami K, Takeda H, Kawakami N, Kobayashi M, Matsuda N, Mishina M. A
1042 Transposon-Mediated Gene Trap Approach Identifies Developmentally Regulated Genes
1043 in Zebrafish. Developmental Cell. 2004;7: 133–144. doi:10.1016/j.devcel.2004.06.005

1044 72. Kim JH, Lee S-R, Li L-H, Park H-J, Park J-H, Lee KY, et al. High Cleavage Efficiency of a
1045 2A Peptide Derived from Porcine Teschovirus-1 in Human Cell Lines, Zebrafish and Mice.
1046 PLOS ONE. 2011;6: e18556. doi:10.1371/journal.pone.0018556

1047 73. Liu Z, Chen O, Wall JBJ, Zheng M, Zhou Y, Wang L, et al. Systematic comparison of 2A
1048 peptides for cloning multi-genes in a polycistronic vector. Scientific Reports. 2017;7:
1049 2193. doi:10.1038/s41598-017-02460-2

1050 74. Mosimann C, Kaufman CK, Li P, Pugach EK, Tamplin OJ, Zon LI. Ubiquitous transgene
1051 expression and Cre-based recombination driven by the ubiquitin promoter in zebrafish.
1052 Development. 2011;138: 169–177. doi:10.1242/dev.059345

1053 75. Ueda Y, Mizuno N, Araki M. Transgenic Xenopus laevis with the ef1-α promoter as an
1054 experimental tool for amphibian retinal regeneration study. genesis. 2012;50: 642–650.
1055 doi:10.1002/dvg.22024

1056 76. Wootton RJ. A Functional Biology of Sticklebacks. 1st ed. University of California Press;
1057 1984. doi:10.2307/jj.8306147

1058 77. Varadharajan S, Rastas P, Löytynoja A, Matschiner M, Calboli FCF, Guo B, et al. A High-
1059 Quality Assembly of the Nine-Spined Stickleback (Pungitius pungitius) Genome. Genome
1060 Biology and Evolution. 2019;11: 3291–3308. doi:10.1093/gbe/evz240

1061 78. Bachtrog D. Y-chromosome evolution: emerging insights into processes of Y-chromosome
1062 degeneration. Nat Rev Genet. 2013;14: 113–124. doi:10.1038/nrg3366

1063 79. Swarup H. Stages in the Development of the Stickleback Gasterosteus aculeatus (L.).
1064 Development. 1958;6: 373–383.

1065 80. Lewis ZR, McClellan MC, Postlethwait JH, Cresko WA, Kaplan RH. Female-specific
1066 increase in primordial germ cells marks sex differentiation in threespine stickleback (
1067 *Gasterosteus aculeatus*). J Morphol. 2008;269: 909–921. doi:10.1002/jmor.10608

1068 81. Shi D-L. Interplay of RNA-binding proteins controls germ cell development in zebrafish.
1069 Journal of Genetics and Genomics. 2024;51: 889–899. doi:10.1016/j.jgg.2024.06.020

1070 82. Planells B, Gómez-Redondo I, Pericuesta E, Lonergan P, Gutiérrez-Adán A. Differential
1071 isoform expression and alternative splicing in sex determination in mice. BMC Genomics.
1072 2019;20: 202. doi:10.1186/s12864-019-5572-x

1073 83. He W, Gauri M, Li T, Wang R, Lin S-X. Current knowledge of the multifunctional 17β-
1074 hydroxysteroid dehydrogenase type 1 (HSD17B1). Gene. 2016;588: 54–61.
1075 doi:10.1016/j.gene.2016.04.031

1076 84. Koyama T, Nakamoto M, Morishima K, Yamashita R, Yamashita T, Sasaki K, et al. A SNP
1077 in a Steroidogenic Enzyme Is Associated with Phenotypic Sex in Seriola Fishes. Current
1078 Biology. 2019;29: 1901-1909.e8. doi:10.1016/j.cub.2019.04.069

1079 85. Desaulniers AT, Cederberg RA, Lents CA, White BR. Expression and Role of
1080 Gonadotropin-Releasing Hormone 2 and Its Receptor in Mammals. Front Endocrinol.
1081 2017;8. doi:10.3389/fendo.2017.00269

1082 86. Sarraj MA, Sarraj ,Mai A., Chua ,Hui Kheng, Sarraj ,Mai A., Chua ,Hui Kheng, Umbers
1083 ,Alexandra, et al. Differential expression of TGFBR3 (betaglycan) in mouse ovary and
1084 testis during gonadogenesis. Growth Factors. 2007;25: 334–345.
1085 doi:10.1080/08977190701833619

1086 87. Wickramasinghe D, Becker S, Ernst MK, Resnick JL, Centanni JM, Tessarollo L, et al.
1087 Two CDC25 homologues are differentially expressed during mouse development.
1088 Development. 1995;121: 2047–2056. doi:10.1242/dev.121.7.2047

1089 88. Namgoong S, Kim N-H. Meiotic spindle formation in mammalian oocytes: implications for
1090 human infertility†. Biology of Reproduction. 2018;98: 153–161. doi:10.1093/biolre/iox145

1091 89. Strüssmann CA, Saito T, Usui M, Yamada H, Takashima F. Thermal thresholds and critical
1092 period of thermolabile sex determination in two atherinid fishes, Odontesthes bonariensis
1093 and Patagonina hatcheri. Journal of Experimental Zoology. 1997;278: 167–177.
1094 doi:10.1002/(SICI)1097-010X(19970615)278:3<167::AID-JEZ6>3.0.CO;2-M

1095 90. Baroiller JF, D'Cotta H, Bezault E, Wessels S, Hoerstgen-Schwark G. Tilapia sex
1096 determination: Where temperature and genetics meet. Comparative Biochemistry and
1097 Physiology Part A: Molecular & Integrative Physiology. 2009;153: 30–38.
1098 doi:10.1016/j.cbpa.2008.11.018

1099 91. Sun P, You F, Ma D, Li J, Zhang P. Sex steroid changes during temperature-induced
1100 gonadal differentiation in (Temminck & Schegel, 1846). Journal of Applied Ichthyology.
1101 2013;29: 886–890. doi:10.1111/jai.12128

1102 92. Borg B, van den Hurk R. Oocytes in the Testes of the Three-Spined Stickleback,
1103 Gasterosteus aculeatus. Copeia. 1983;1983: 259–261. doi:10.2307/1444727

1104 93. Gercken J, Sordyl H. Intersex in feral marine and freshwater fish from northeastern
1105 Germany. Marine Environmental Research. 2002;54: 651–655. doi:10.1016/S0141-
1106 1136(02)00156-3

1107 94. Aharon D, Marlow FL. Sexual determination in zebrafish. Cell Mol Life Sci. 2021;79: 8.
1108 doi:10.1007/s00018-021-04066-4

1109 95. Slanchev K, Stebler J, de la Cueva-Méndez G, Raz E. Development without germ cells:
1110 The role of the germ line in zebrafish sex differentiation. Proceedings of the National
1111 Academy of Sciences. 2005;102: 4074–4079. doi:10.1073/pnas.0407475102

1112 96. Tzung K-W, Goto R, Saju JM, Sreenivasan R, Saito T, Arai K, et al. Early Depletion of
1113 Primordial Germ Cells in Zebrafish Promotes Testis Formation. Stem Cell Reports.
1114 2015;4: 61–73. doi:10.1016/j.stemcr.2014.10.011

1115 97. Schartl M. A comparative view on sex determination in medaka. Mechanisms of
1116 Development. 2004;121: 639–645. doi:10.1016/j.mod.2004.03.001

1117 98. Kurokawa H, Saito D, Nakamura S, Katoh-Fukui Y, Ohta K, Baba T, et al. Germ cells are
1118 essential for sexual dimorphism in the medaka gonad. Proceedings of the National
1119 Academy of Sciences. 2007;104: 16958–16963. doi:10.1073/pnas.0609932104

1120 99. Nakamura S, Watakabe I, Nishimura T, Picard J-Y, Toyoda A, Taniguchi Y, et al.
1121 Hyperproliferation of mitotically active germ cells due to defective anti-Müllerian hormone
1122 signaling mediates sex reversal in medaka. Development. 2012;139: 2283–2287.
1123 doi:10.1242/dev.076307

1124 100. Tezak B, Straková B, Fullard DJ, Dupont S, McKey J, Weber C, et al. Higher
1125 temperatures directly increase germ cell number, promoting feminization of red-eared
1126 slider turtles. Current Biology. 2023;0. doi:10.1016/j.cub.2023.06.008

1127 101. Lyet L, Louis F, Forest MG, Josso N, Behringer RR, Vigier B. Ontogeny of Reproductive
1128 Abnormalities Induced by Deregulation of Anti-Müllerian Hormone Expression in

Transgenic Mice. Biology of Reproduction. 1995;52: 444–454. doi:10.1095/biolreprod52.2.444

102. Han Y, Zhao M, Wang L, Yu Z, Wang J, Yu Q, et al. Overexpression of Anti-müllerian Hormone Gene in vivo Affects Gonad Sex Differentiation in Undifferentiated Orange-Spotted Groupers (Epinephelus coioides). Front Endocrinol. 2019;0. doi:10.3389/fendo.2019.00210

103. Rehman Z ur, Worku T, Davis JS, Talpur HS, Bhattarai D, Kadariya I, et al. Role and mechanism of AMH in the regulation of Sertoli cells in mice. The Journal of Steroid Biochemistry and Molecular Biology. 2017;174: 133–140. doi:10.1016/j.jsbmb.2017.08.011

104. Rodriguez KF, Brown PR, Amato CM, Nicol B, Liu C-F, Xu X, et al. Somatic cell fate maintenance in mouse fetal testes via autocrine/paracrine action of AMH and activin B. Nat Commun. 2022;13: 4130. doi:10.1038/s41467-022-31486-y

105. Guiguen Y, Fostier A, Piferrer F, Chang C-F. Ovarian aromatase and estrogens: A pivotal role for gonadal sex differentiation and sex change in fish. General and Comparative Endocrinology. 2010;165: 352–366. doi:10.1016/j.ygcen.2009.03.002

106. Li M, Sun L, Wang D. Roles of estrogens in fish sexual plasticity and sex differentiation. General and Comparative Endocrinology. 2019;277: 9–16. doi:10.1016/j.ygcen.2018.11.015

107. Liu X, Dai S, Wu J, Wei X, Zhou X, Chen M, et al. Roles of anti-Müllerian hormone and its duplicates in sex determination and germ cell proliferation of Nile tilapia. Genetics. 2021; iyab237. doi:10.1093/genetics/iyab237

108. Halm S, Rocha A, Miura T, Prat F, Zanuy S. Anti-Müllerian hormone (*AMH*/AMH) in the European sea bass: Its gene structure, regulatory elements, and the expression of alternatively-spliced isoforms. Gene. 2007;388: 148–158. doi:10.1016/j.gene.2006.10.018

109. Liu X, Xiao H, Jie M, Dai S, Wu X, Li M, et al. Amh regulate female folliculogenesis and fertility in a dose-dependent manner through Amhr2 in Nile tilapia. Molecular and Cellular Endocrinology. 2020;499: 110593. doi:10.1016/j.mce.2019.110593

110. Wu K, Yue Y, Zhou L, Zhang Z, Shan H, He H, et al. Disrupting Amh and androgen signaling reveals their distinct roles in zebrafish gonadal differentiation and gametogenesis. Commun Biol. 2025;8: 1–15. doi:10.1038/s42003-025-07719-3

111. Zhang Z, Wu K, Ren Z, Ge W. Genetic evidence for Amh modulation of gonadotropin actions to control gonadal homeostasis and gametogenesis in zebrafish and its noncanonical signaling through Bmpr2a receptor. Development. 2020;147: dev189811. doi:10.1242/dev.189811

112. Ijiri S, Kaneko H, Kobayashi T, Wang D-S, Sakai F, Paul-Prasanth B, et al. Sexual Dimorphic Expression of Genes in Gonads During Early Differentiation of a Teleost Fish, the Nile Tilapia Oreochromis niloticus1. Biology of Reproduction. 2008;78: 333–341. doi:10.1095/biolreprod.107.064246

113. Czerwinski M, Natarajan A, Barske L, Looger LL, Capel B. A timecourse analysis of systemic and gonadal effects of temperature on sexual development of the red-eared slider turtle Trachemys scripta elegans. Developmental Biology. 2016;420: 166–177. doi:10.1016/j.ydbio.2016.09.018

114. Sánchez-Baizán N, Jarne-Sanz I, Roco ÁS, Schartl M, Piferrer F. Extraordinary variability in gene activation and repression programs during gonadal sex differentiation across vertebrates. Front Cell Dev Biol. 2024;12. doi:10.3389/fcell.2024.1328365

115. Hacker A, Capel B, Goodfellow P, Lovell-Badge R. Expression of Sry, the mouse sex determining gene. Development. 1995;121: 1603–1614. doi:10.1242/dev.121.6.1603

116. Kobayashi T, Nagahama Y. Molecular Aspects of Gonadal Differentiation in a Teleost Fish, the Nile Tilapia. Sexual Development. 2009;3: 108–117. doi:10.1159/000223076

117. Eshel O, Shirak A, Weller JI, Hulata G, Ron M. Linkage and Physical Mapping of Sex Region on LG23 of Nile Tilapia (Oreochromis niloticus). G3 Genes|Genomes|Genetics. 2012;2: 35–42. doi:10.1534/g3.111.001545

118. Liu X, Zhou L, Li W, Zhang L, Li M, Wang D. Production of fertile YY pseudofemales in Nile tilapia with LG23 as the sex chromosome. Aquaculture. 2024;587: 740870. doi:10.1016/j.aquaculture.2024.740870

119. Yamazaki W, Tan SL, Taketo T. Role of the X and Y Chromosomes in the Female Germ Cell Line Development in the Mouse (Mus musculus). Sexual Development. 2023;16: 355–364. doi:10.1159/000521151

120. Lam TJ, Nagahama Y, Chan K, Hoar WS. Overripe eggs and postovulatory corpora lutea in the threespine stickleback, Gasterosteus aculeatus L., form trachurus. Can J Zool. 1978;56: 2029–2036. doi:10.1139/z78-273

121. Roufidou C, Sebire M, Katsiadaki I, Mustafa A, Schmitz M, Mayer I, et al. Overripening of eggs and changes in reproductive hormones in the threespine stickleback, Gasterosteus aculeatus. Evol Ecol Res. 2016;17: 583–601.

122. Roufidou C, Borg B. Ovarian fluid in the three-spined stickleback : effects of egg overripening and sex steroid treatment. Journal of Fish Biology. 2019;94: 446–457. doi:10.1111/jfb.13915

123. Levy ER, Burgoyne PS. The fate of XO germ cells in the testes of XO/XY and XO/XY/XYY mouse mosaics: evidence for a spermatogenesis gene on the mouse Y chromosome. Cytogenet Cell Genet. 1986;42: 208–213. doi:10.1159/000132280

124. Mazeyrat S, Saut N, Grigoriev V, Mahadevaiah SK, Ojarikre OA, Rattigan Á, et al. A Y-encoded subunit of the translation initiation factor Eif2 is essential for mouse spermatogenesis. Nat Genet. 2001;29: 49–53. doi:10.1038/ng717

125. Touré A, Szot M, Mahadevaiah SK, Rattigan A, Ojarikre OA, Burgoyne PS. A new deletion of the mouse Y chromosome long arm associated with the loss of Ssty expression, abnormal sperm development and sterility. Genetics. 2004;166: 901–912.

126. Vernet N, Mahadevaiah SK, Yamauchi Y, Decarpentrie F, Mitchell MJ, Ward MA, et al. Mouse Y-Linked Zfy1 and Zfy2 Are Expressed during the Male-Specific Interphase between Meiosis I and Meiosis II and Promote the 2nd Meiotic Division. PLOS Genetics. 2014;10: e1004444. doi:10.1371/journal.pgen.1004444

127. Yamauchi Y, Riel JM, Stoytcheva Z, Ward MA. Two Y Genes Can Replace the Entire Y Chromosome for Assisted Reproduction in the Mouse. Science. 2014;343: 69–72. doi:10.1126/science.1242544

128. Shaw DE, Ross WD, Lambert AV, White MA. Single cell RNA-sequencing reveals no evidence for meiotic sex chromosome inactivation in the threespine stickleback fish. bioRxiv; 2024. p. 2024.11.26.625488. doi:10.1101/2024.11.26.625488

129. Largiadèr CR, Fries V, Bakker TCM. Genetic analysis of sneaking and egg-thievery in a natural population of the three-spined stickleback (Gasterosteus aculeatus L.). Heredity. 2001;86: 459–468. doi:10.1046/j.1365-2540.2001.00850.x

130. Mehlis M, Rahn AK, Bakker TCM. Sperm quality but not relatedness predicts sperm competition success in threespine sticklebacks (Gasterosteus aculeatus). BMC Evol Biol. 2015;15: 74. doi:10.1186/s12862-015-0353-x

131. Mehlis M, Hilke LK, Bakker TCM. Attractive males have faster sperm in three-spined sticklebacks Gasterosteus aculeatus. Current Zoology. 2013;59: 761–768. doi:10.1093/czoolo/59.6.761

132. Arnold AP, Chen X. What does the “four core genotypes” mouse model tell us about sex differences in the brain and other tissues? Frontiers in Neuroendocrinology. 2009;30: 1–9. doi:10.1016/j.yfrne.2008.11.001

133. Arnold AP. Four Core Genotypes and XY* mouse models: Update on impact on SABV research. Neuroscience & Biobehavioral Reviews. 2020;119: 1–8. doi:10.1016/j.neubiorev.2020.09.021

134. Vries GJD, Rissman EF, Simerly RB, Yang L-Y, Scordalakes EM, Auger CJ, et al. A Model System for Study of Sex Chromosome Effects on Sexually Dimorphic Neural and Behavioral Traits. J Neurosci. 2002;22: 9005–9014. doi:10.1523/JNEUROSCI.22-20-09005.2002

135. Gatewood JD, Wills A, Shetty S, Xu J, Arnold AP, Burgoyne PS, et al. Sex Chromosome Complement and Gonadal Sex Influence Aggressive and Parental Behaviors in Mice. J Neurosci. 2006;26: 2335–2342. doi:10.1523/JNEUROSCI.3743-05.2006

136. Suster ML, Abe G, Schouw A, Kawakami K. Transposon-mediated BAC transgenesis in zebrafish. Nat Protoc. 2011;6: 1998–2021. doi:10.1038/nprot.2011.416

137. Montague TG, Cruz JM, Gagnon JA, Church GM, Valen E. CHOPCHOP: a CRISPR/Cas9 and TALEN web tool for genome editing. Nucleic Acids Research. 2014;42: W401–W407. doi:10.1093/nar/gku410

138. Labun K, Montague TG, Gagnon JA, Thyme SB, Valen E. CHOPCHOP v2: a web tool for the next generation of CRISPR genome engineering. Nucleic Acids Research. 2016;44: W272–W276. doi:10.1093/nar/gkw398

139. Labun K, Montague TG, Krause M, Torres Cleuren YN, Tjeldnes H, Valen E. CHOPCHOP v3: expanding the CRISPR web toolbox beyond genome editing. Nucleic Acids Research. 2019;47: W171–W174. doi:10.1093/nar/gkz365

140. Subedi A, Macurak M, Gee ST, Monge E, Goll MG, Potter CJ, et al. Adoption of the Q transcriptional regulatory system for zebrafish transgenesis. Methods. 2014;66: 433–440. doi:10.1016/j.ymeth.2013.06.012

141. Kingsley DM, Zhu B, Osoegawa K, De Jong PJ, Schein J, Marra M, et al. New Genomic Tools for Molecular Studies of Evolutionary Change in Threespine Sticklebacks. Behaviour. 2004;141: 1331–1344.

142. Archambeault SL, Bärtschi LR, Merminod AD, Peichel CL. Adaptation via pleiotropy and linkage: Association mapping reveals a complex genetic architecture within the stickleback Eda locus. Evolution Letters. 2020;4: 282–301. doi:10.1002/evl3.175

143. Collins III JJ, Hou X, Romanova EV, Lambrus BG, Miller CM, Saberi A, et al. Genome-Wide Analyses Reveal a Role for Peptide Hormones in Planarian Germline Development. PLOS Biology. 2010;8: e1000509. doi:10.1371/journal.pbio.1000509

144. Square TA, Sundaram S, Mackey EJ, Miller CT. Distinct tooth regeneration systems deploy a conserved battery of genes. EvoDevo. 2021;12: 4. doi:10.1186/s13227-021-00172-3

145. Edgar RC. Muscle5: High-accuracy alignment ensembles enable unbiased assessments of sequence homology and phylogeny. Nat Commun. 2022;13: 6968. doi:10.1038/s41467-022-34630-w

146. Paradis E, Schliep K. ape 5.0: an environment for modern phylogenetics and evolutionary analyses in R. Bioinformatics. 2019;35: 526–528. doi:10.1093/bioinformatics/bty633

147. Mayor C, Brudno M, Schwartz JR, Poliakov A, Rubin EM, Frazer KA, et al. VISTA : visualizing global DNA sequence alignments of arbitrary length. Bioinformatics. 2000;16: 1046–1047. doi:10.1093/bioinformatics/16.11.1046

148. Frazer KA, Pachter L, Poliakov A, Rubin EM, Dubchak I. VISTA: computational tools for comparative genomics. Nucleic Acids Research. 2004;32: W273–W279. doi:10.1093/nar/gkh458

149. Brudno M, Do CB, Cooper GM, Kim MF, Davydov E, Program NCS, et al. LAGAN and Multi-LAGAN: Efficient Tools for Large-Scale Multiple Alignment of Genomic DNA. Genome Res. 2003;13: 721–731. doi:10.1101/gr.926603

150. Bolger AM, Lohse M, Usadel B. Trimmomatic: a flexible trimmer for Illumina sequence data. Bioinformatics. 2014;30: 2114–2120. doi:10.1093/bioinformatics/btu170

151. Zhang Y, Park C, Bennett C, Thornton M, Kim D. Rapid and accurate alignment of nucleotide conversion sequencing reads with HISAT-3N. Genome Res. 2021;31: 1290–1295. doi:10.1101/gr.275193.120

152. Putri GH, Anders S, Pyl PT, Pimanda JE, Zanini F. Analysing high-throughput sequencing data in Python with HTSeq 2.0. Bioinformatics. 2022;38: 2943–2945. doi:10.1093/bioinformatics/btac166

153. Love MI, Huber W, Anders S. Moderated estimation of fold change and dispersion for RNA-seq data with DESeq2. Genome Biology. 2014;15: 550. doi:10.1186/s13059-014-0550-8

1290 **Supplemental figures and tables**
1291

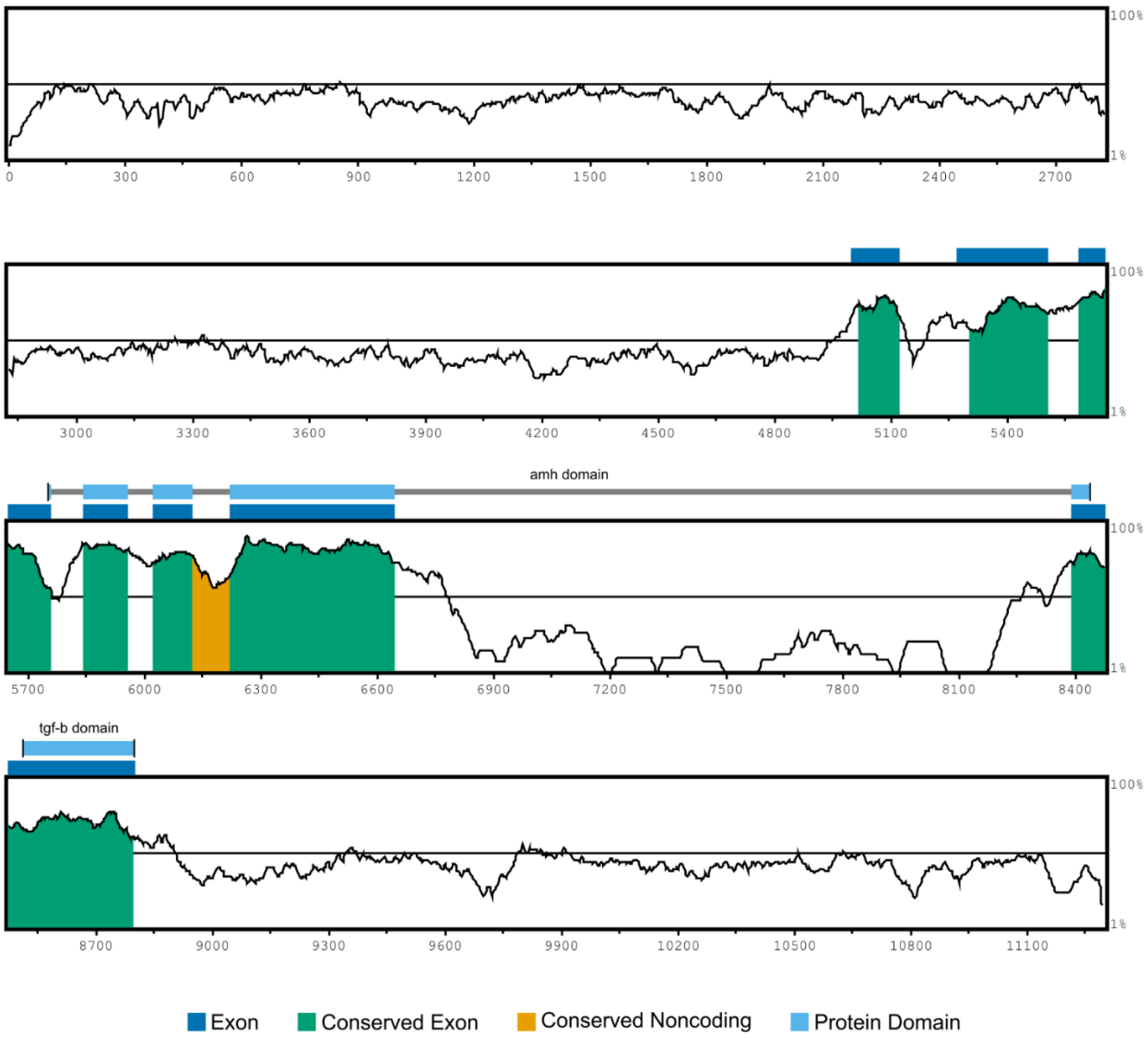

1292
1293 Fig S1. Sequence conservation of the *amhy* transgene region with autosomal *amha*.
1294 Vistaplot showing conserved sequence identity of *amhy* to *amha* with sequence identity on the Y
1295 axis and base pair position of *amhy* on the x axis. Exon positions are indicated in dark blue, and
1296 the amh domain and TGF-β domain are indicated in light blue above the graph. Conserved
1297 sequences share 70% sequence identity in a 100 bp window.
1298

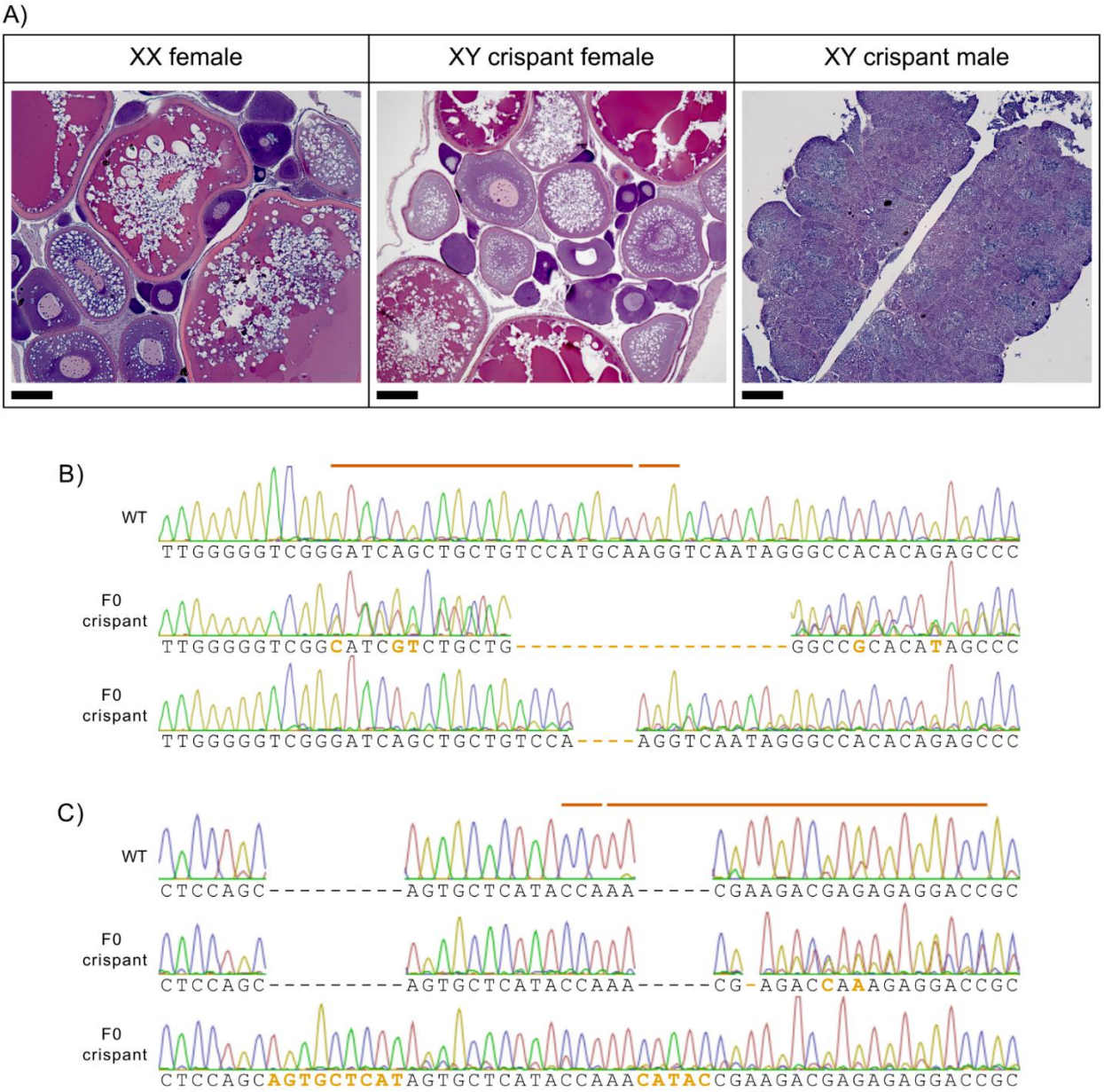

Fig S2. F0 *amhy* crispants show genetic mosaicism and variable sex reversal
A) XY crispants developed as females with ovaries or males with testes. Sanger sequencing of exon 1 (B) and exon 3 (C) show various mutations relative to wildtype. Discordant chromatograms in crispants are indicative of mosaic mutations. Mutations are bolded in orange. CRISPR target site and PAM sequence are indicated by orange lines above wildtype reference sequence.

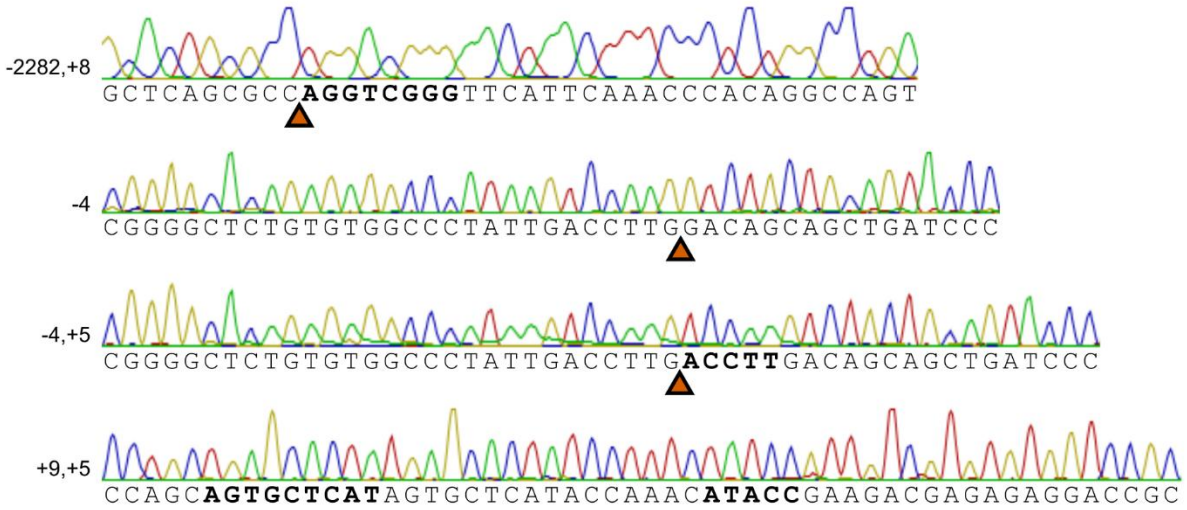

Fig S3. Sanger sequencing of four F1 *amhy* mutant alleles.
Inserted base pairs are bolded. Locations of deletions are indicated with red arrowheads.

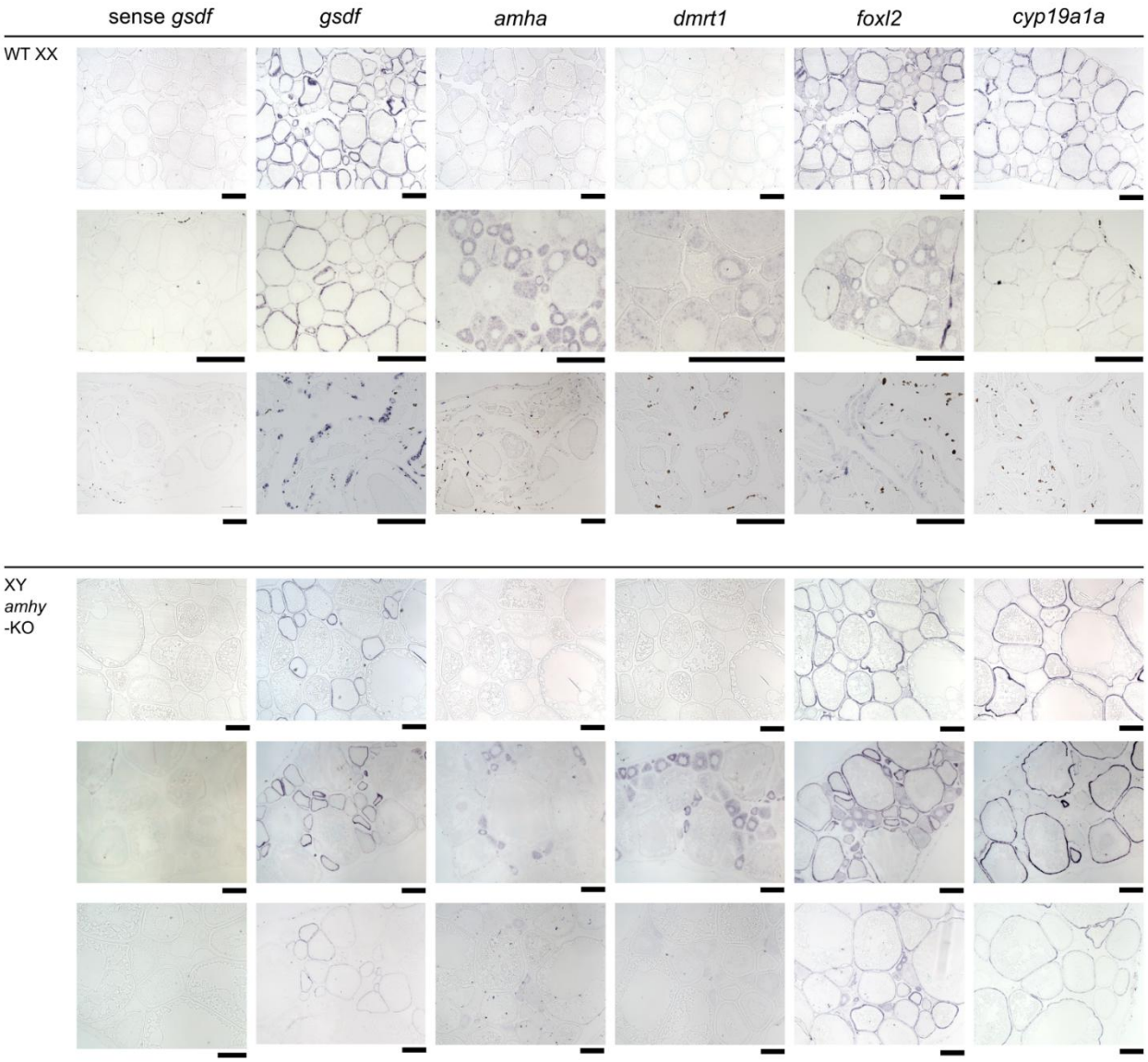

Fig S4. Expression of gonadal genes in wildtype and sex reversed ovaries
In situ hybridization of gonadal genes in three biological replicates for wildtype XX ovaries and XY *amhy*-KO ovaries. Scale bars = 200 μm.

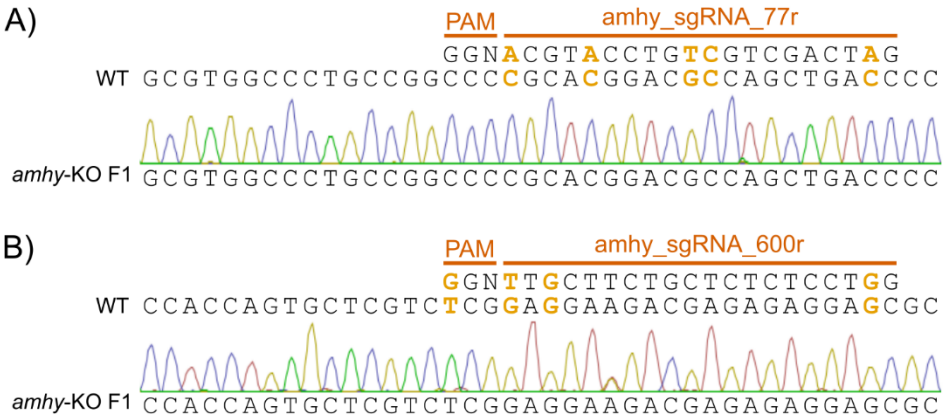

Fig S5. CRISPR/Cas9 sgRNAs for *amhy* have multiple mismatches to their homologous site in *amha*.
PAM and sgRNA sequences are shown above the reference sequence. Mismatched nucleotides are bolded in orange text. Sanger sequencing of sex reversed XY F1 *amhy*-KO fish showed no off-target mutations in *amha* in exon 1 (A) or exon 3 (B).

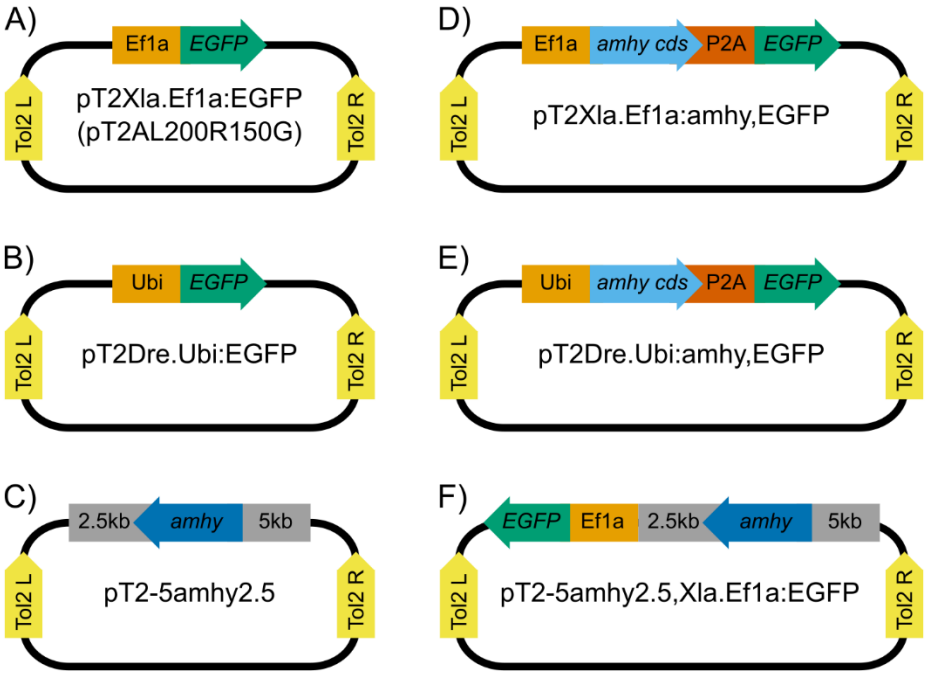

Fig S6. Plasmid maps of transgenes constructed in this study.
Transgenes used the *X. laevis* Ef1a promoter (A and D), *D. rerio* Ubi promoter (B and E), or endogenous *amhy* promoter (C and F). Control transgenes express only EGFP (A and B). Other transgenes contain the *amhy* coding sequence (D and E) or the full *amhy* sequence including introns (C and F). To screen for transgene integration, *amhy* transgenes include an EGFP joined to *amhy* with a P2A self-cleaving peptide (D and E) or separate EGFP cassette (F). All transgenes are flanked by Tol2 transposon arms to facilitate transgene integration.

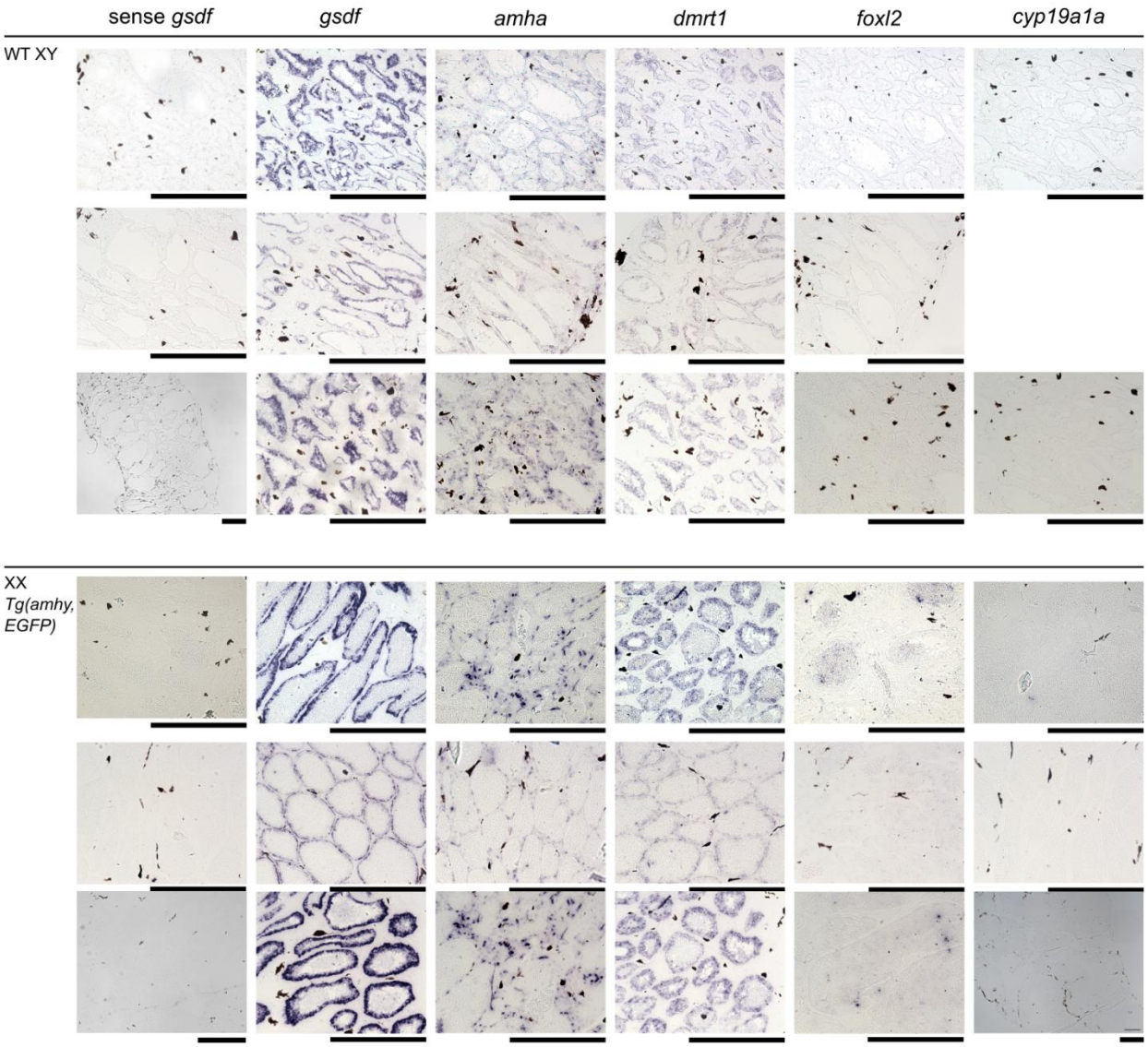

Fig S7. Expression of gonadal genes in wildtype and sex reversed testes.
In situ hybridization of gonadal genes in three biological replicates for wildtype XY testes and XX *Tg(amhy,EGFP)* testes. For one wildtype replicate, the tissue was lost during staining for *cyp19a1a*. Scale bars = 200 µm.

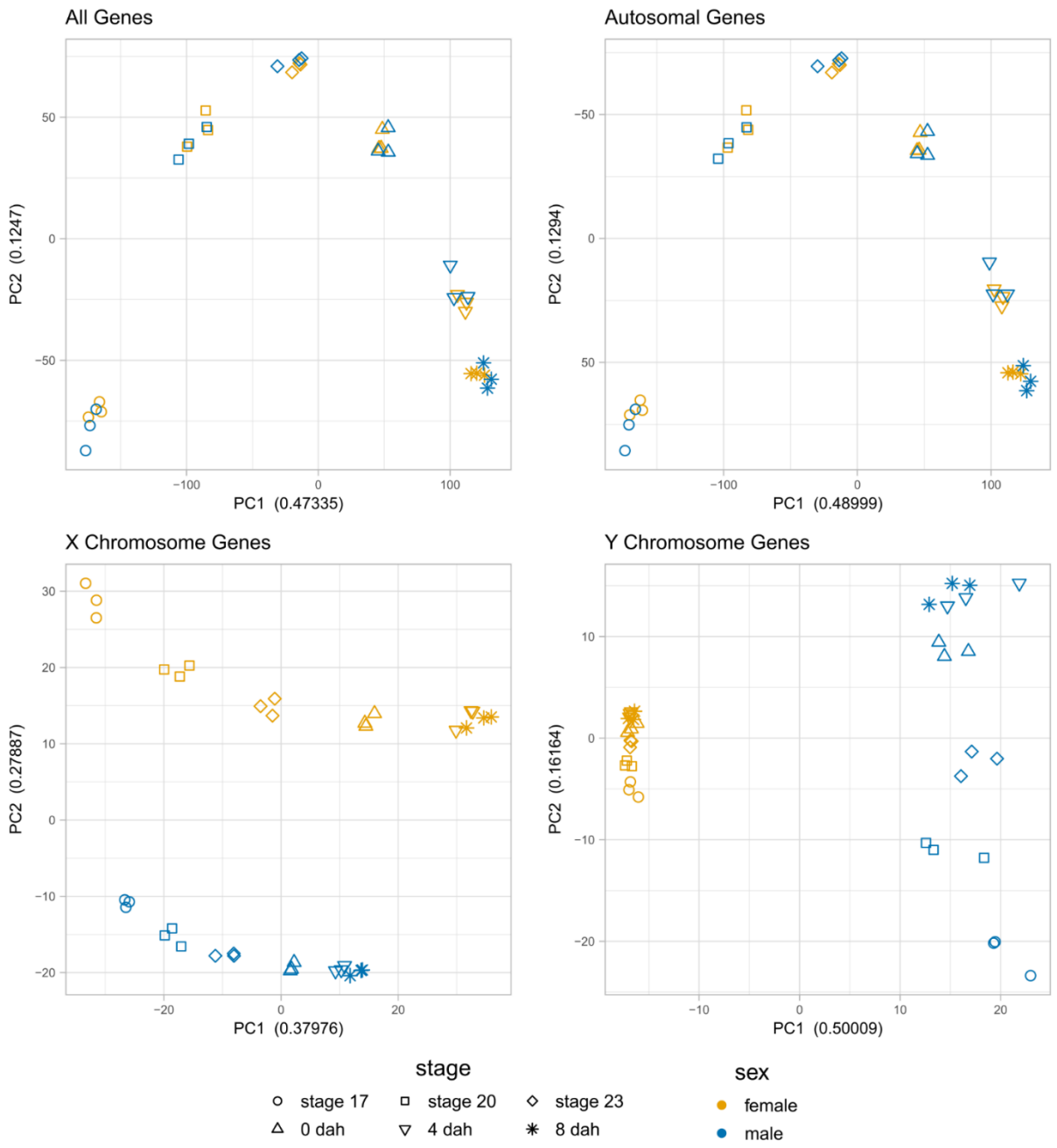

Fig S8. PCA plots of normalized gene expression counts.
Principal components 1 and 2 with the Proportion of Variance Explained on the X and Y axes, respectively. When analyzing all genes or autosomal genes only, samples group by developmental stage and not sex. X chromosome genes show separation by both stage and sex. Y chromosome genes group primarily by sex with male samples separate by developmental stage.

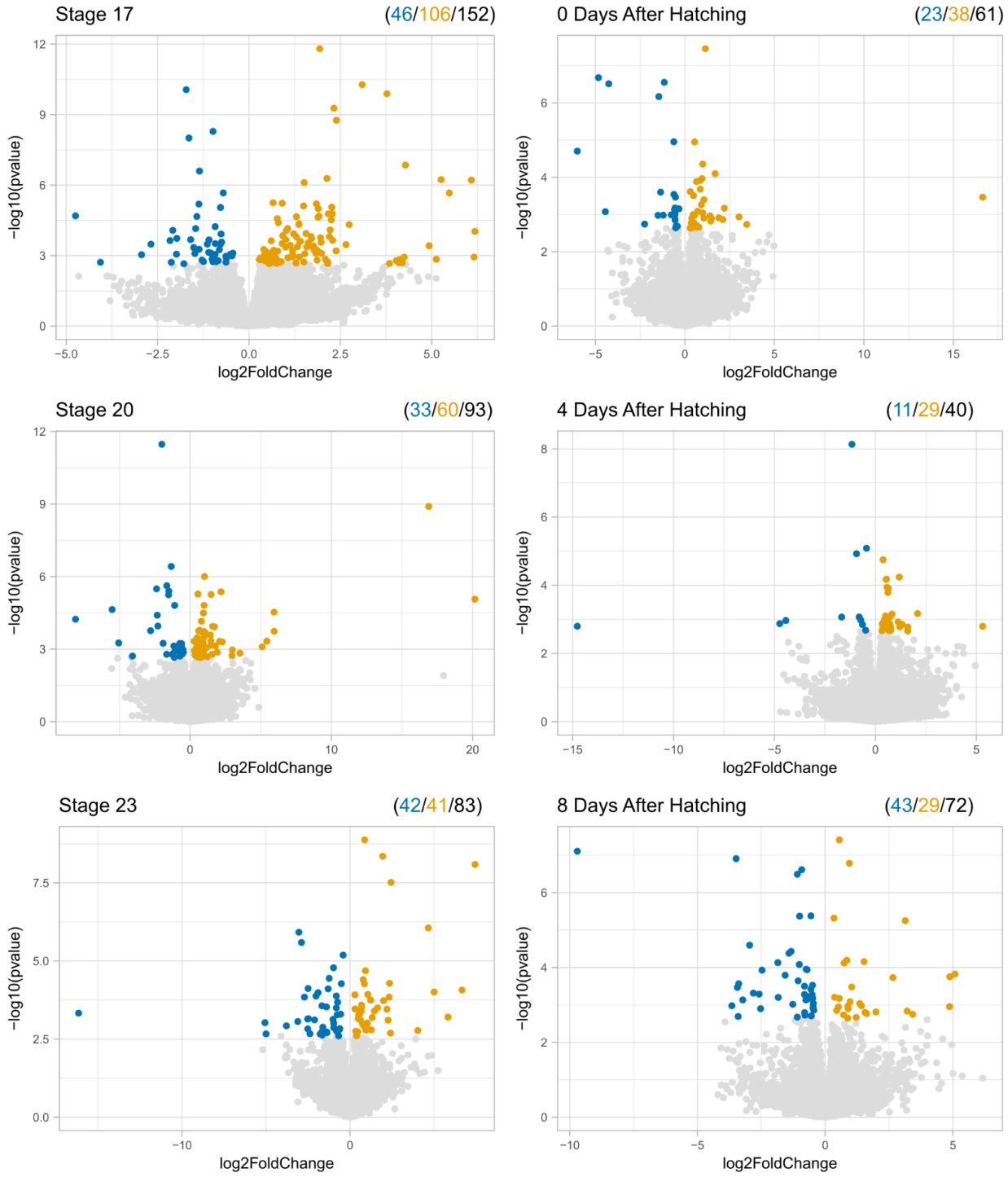

Fig S9. Volcano plots of female to male differential expression by stage. Positive log2 Fold Change values indicate higher expression in females, and negative values indicate higher expression in males. Significant genes (adjusted $p < 0.05$) are shaded. The number of male biased, female biased, and total differentially expressed genes are shown above each plot.

Table S1. Viability and Hatching rates of crosses from F1 XY *amhy*-KO females with wildtype XY males

Fish	Cross number	Clutch Size	Viable	Hatched	Viable:total	Hatched:total	Hatched:viable
A	1	43	1	1	0.0233	0.0233	1.0000
B	1	51	2	0	0.0392	0.0000	0.0000
C	1	63	4	2	0.0635	0.0317	0.5000
C	2	99	24	21	0.2424	0.2121	0.8750
C	3	81	11	6	0.1358	0.0741	0.5455
C	4	100	78	54	0.7800	0.5400	0.6923
C	5	89	70	46	0.7865	0.5169	0.6571

Table S2. Viability and Hatching rates of crosses from F2 XX or XY *amhy*-KO females a wildtype XY male

Genotype	Clutch Size	Viable	Hatched	Viable:total	Hatched:total	Hatched:viable
XX	57	57	57	1.0000	1.0000	1.0000
XX	112	105	34	0.9375	0.3036	0.3238
XX	56	55	55	0.9821	0.9821	1.0000
XX	136	90	47	0.6618	0.3456	0.5222
XX	94	94	79	1.0000	0.8404	0.8404
XY	84	6	2	0.0714	0.0238	0.3333
XY	65	0	0	0.0000	0.0000	NA
XY	98	0	0	0.0000	0.0000	NA
XY	22	0	0	0.0000	0.0000	NA
XY	72	6	4	0.0833	0.0556	0.6667
XY	92	0	0	0.0000	0.0000	NA
Total XX	455	401	272	0.8813	0.5978	0.6783
Total XY	433	12	6	0.0277	0.0139	0.5000

Table S3. Combined *amha* and *amhy* expression show no significant difference between males and females

stage	stage 17		stage 20		stage 23		0 dah		4 dah		8 dah	
sex	female	male	female	male	female	male	female	male	female	male	female	male
amha normalized counts	24.2	31.0	32.5	62.5	142.8	98.1	250.9	248.8	314.6	408.4	348.0	350.2
	35.3	13.2	48.5	37.4	125.2	57.8	288.3	286.2	395.5	286.7	407.7	493.6
	27.5	28.4	54.0	33.1	98.0	109.8	283.8	331.6	318.2	364.8	525.1	431.9
Mean	29.0	24.2	45.0	44.3	122.0	88.6	274.3	288.9	342.8	353.3	426.9	425.2
SD	5.7	9.6	11.2	15.9	22.6	27.3	20.4	41.5	45.7	61.7	90.1	71.9
amhy normalized counts	0	9.4	1.0	3.8	0	14.5	0.9	22.5	0	40.8	0	13.5
	0	10.2	0	4.7	0	13.8	0	20.9	0	20.5	0	32.9
	0	5.7	0	5.2	0	13.0	2.9	8.7	0	16.3	0	9.4
Mean	0	8.4	0.3	4.5	0	13.8	1.3	17.4	0	25.9	0	18.6
sd	0	2.4	0.6	0.7	0	0.8	1.5	7.5	0	13.1	0	12.6
length adjusted *amhy* counts	0	9.38	1.01	3.79	0	14.50	0.85	22.50	0	40.84	0	13.54
	0	10.18	0	4.68	0	13.79	0	20.94	0	20.48	0	32.90
	0	5.68	0	5.17	0	12.96	2.93	8.73	0	16.27	0	9.39
Mean	0	8.42	0.34	4.55	0	13.75	1.26	17.39	0	25.86	0	18.61
SD	0	2.40	0.59	0.70	0	0.77	1.50	7.54	0	13.14	0	12.55
amha + adj. *amhy* normalized counts	24.21	45.59	34.06	68.43	142.76	120.73	252.26	283.91	314.60	472.16	348.00	371.36
	35.34	29.13	48.55	44.72	125.18	79.29	288.27	318.92	395.50	318.66	407.67	544.90
	27.52	37.28	54.01	41.15	97.97	130.05	288.35	345.21	318.15	390.16	525.11	446.56
Mean	29.02	37.33	45.54	51.44	121.97	110.02	276.29	316.01	342.75	393.66	426.93	454.27
SD	5.71	8.23	10.31	14.82	22.57	27.02	20.81	30.75	45.72	76.81	90.11	87.03
P value	0.4078		0.6054		0.5892		0.1474		0.3913		0.7246	

Length adjusted *amhy* counts were calculated by multiplying *amhy* normalized read counts by transcript length of *amha* (3895 bp) divided by *amhy* (2496 bp). P values show two tailed t test for difference in total *amh* expression between males and females at each stage ($P < 0.05$)

1368 Table S4 – PCR primers used in this study

Assay	Forward primer	Reverse primer
XY *idh* genotyping	5'-GGGACGAGCAAGATTTATT-3'	5'-TTATCGTTAGCCAGGAGATGG-3'
Amhy exon 1 genotyping, amhy transgene detection	5'-TTGGTGGGTTGATGCTCTGC-3'	5'-CTATGTGAGAGACTGTGGCGG-3'
amhy exon 3 genotyping	5'-TCAGTTTGGAATCTGCACTGTT-3'	5'-GGATGCAGTGATTTACTGGTGA-3'
amhy 2.3 kb deletion genotyping	5'-CACAGTCCTTCGACTCCTTCG-3'	5'-GAGACCATGGTGACTGGCTC-3'
amha exon 1 genotyping	5'-GGCAGTGAGAAGGGAAGGTG-3'	5'-GGCCTCTGGTGATGGGAATG-3'
amha exon 3 genotyping	5'-CAGCCGGAGTCAGTTTGGAA-3'	5'-TCATGCATCGTCGACTGGAG-3'
EGFP transgene detection	5'-ATCATGGCCGACAAGCAGAA-3'	5'-AACTCCAGCAGGACCATGTG-3'
Dmrt1 riboprobe cloning	5'-AGCAGCACCGAGAAGCAG-3'	5'-CTCGTTGACGTTGCCCATGA-3'
Gsdf riboprobe cloning	5'-TTTTGTCACGGCGATGCTTC-3'	5'-AGGAAATGACGAGGGTGCTG-3'
Foxl2 riboprobe cloning	5'-GAGAAGGTCCCGGAGAAAGC-3'	5'-GCAGTGCATCATCGAGAGCT-3'
Cyp19a1a riboprobe cloning	5'-CCTTGTTTCTGTCTGGGCCT-3'	5'-TTGAGGAGCAGCAGCATGA-3'
Riboprobe template synthesis	5'-TAATACGACTCACTATAGGG-3'	5'-TAATACGACTCACTATAGGG-3'

1369
1370